2011-11-06

Assessment of cardiac autonomic neuropathy (CAN) in Type I diabetic mice

Bufan Yang
Worcester Polytechnic Institute

Assessment of cardiac autonomic neuropathy (CAN) in Type I diabetic mice

Advisor: Dr. Ki H. Chon

Dissertation Committee: Dr. Marsha W. Rolle

Dr. Domhnull Granquist-Fraser

Dr. Bengisu Tulu

Dr. Leon Moore

Dissertation by:

Bufan Yang

Ph.D. Candidate

Department of Biomedical Engineering

bf@wpi.edu

ABSTRACT

Diabetic cardiovascular autonomic neuropathy (DCAN) is common in patients with diabetes mellitus, and causes abnormalities in heart rate control as well as central and peripheral nervous system dynamics. A good understanding of DCAN is not established yet. An effective way to detect diabetes mellitus at an early stage is still undiscovered, and is highly desired by researchers and patients. One reason why the pathogenesis of DCAN is unclear is that non-invasive assessment of DCAN in humans and animals has been problematic. The non-stationary and non-linear natures of the interested physiological signals have placed great limitation on traditional algorithms. To overcome this limitation, this work proposes a series of time-varying, nonlinear and non-invasive methods to assess cardiac autonomic dysregulation from ECG and PPG records. Including a non-stationary method called PDM, which is based on principal dynamic mode (PDM) analysis of heart rate variability (HRV), nonstationary power spectral density called TVOPS-VFCDM and also standard spectrum analysis method of HRV. We are also able to study and analyze a series of long term and short term ECG and PPG data. In a pilot study, ECG was measured via telemetry in conscious 4 month old C57/Bl6 controls and in Akita mice, a model of insulin-dependent type I diabetes, while PPG was measured via tail pulse oximetry from 2 month old to 4 month old. The results indicate significant cardiac autonomic impairment in the diabetic mice in comparison to the controls at 4 month old and such impairment start to present at 3 month old. Further, both immunohistochemistry and Western blot analyses show a reduction in nerve density in Akita mice as compared to the control mice, thus, corroborating our data analysis records.

ACKNOWLEDGEMENT

Foremost, I would like to thank my advisor Prof. Ki H. Chon for the continuous support of my Ph.D study and research. His support, guidance and wisdom walked me through the past few years and turned me into a real researcher. Without his help, I would not have a chance to be part of the state-of-the-art researches of our lab.

Besides my advisor, I would like to thank the rest of my thesis committee: Dr. Marsha Rolle, Dr. Domhnull Granquist-Fraser, Dr. Bengisu Tulu, and Dr. Leon Moore for their encouragement, insightful comments, and thoughtful questions.

Special thanks also goes to Dr. Marsha W. Rolle, Dr. Glenn R. Gaudette, Dr. Christopher Malcuit and Dr. Leon Moore who have help me to carry out the part of protein studies of my thesis work. By the assistance and facility they offered, I had an opportunity to learn some fundamental biology experimental techniques and greatly improve my study.

I thank my fellow lab mates from Dr. Ki H. Chon's lab: Jinseok Lee, Christopher Scully, Nandakumar Selvaraj, Bersain Reyes Jeffery Bolkhovsky , Yan Bai, Kin Lung Siu, Biin Sung, Yuru Zhong, He Zhao, and Sheng Lu; as well as faculties and graduate students from WPI: Sharon Shaw, Dr. Christopher Malcuit, Tracy Gwyther, Jacques Guyette, Olga Kashpur, Denis Kole, and Jonathan Grasman for the stimulating discussions, learning from each other, and for all the fun we have had in the past few years.

Last but not least, I would like to thank my family: my parents Xinquan Yang and Yunqiu Zhang, for giving birth to me at the first place and supporting me all the time throughout my life.

This work is funded by Juvenile Diabetes Research Foundation (JDRF).

TABLE OF CONTENTS

TERMS AND ABBREVIATIONS

DCAN – Diabetic cardiac autonomic neuropathy

CAN – Cardiac autonomic neuropathy

ECG – Electrocardiography

PPG – Photoplethysmograph

HR(V) – Heart rate (variability)

PSD – Power spectrum density

LF – Low frequency

HF – High frequency

RR – R peak to R peak interval

SDNN – Standard deviation of all normal RR intervals

RMSSD – Root of the mean squared difference of successive RR

PDM – Principal dynamic mode

ANS – Autonomic nervous system

SNS – Sympathetic nervous system

PNS – Parasympathetic nervous system

TVOPS – Time varying optimum parameter search

VFCDM – Variable frequency complex demodulation

TH – Tyrosine hydroxylase

Chat – Choline acetyltransferase

LIST OF TABLES AND FIGURES

SPECIFIC AIMS AND HYPOTHESIS

Diabetic cardiovascular autonomic neuropathy (DCAN) is one of the most common complications in patients with diabetes mellitus, and causes abnormalities in the heart rate control as well as the central and peripheral vascular dynamics. Consequences of DCAN include exercise intolerance, intra-operative cardiovascular lability, orthostatic hypotension, and myocardial ischemia. Currently there is no cure for either DCAN or diabetes mellitus, and for most cases, damaged nerves in DCAN is not reversible. The only hope for combating DCAN is to have an early recognition, from which the patients can receive a prompt and sufficient medical care to prevent further deterioration of nerve damage. Moreover, one recent study has reported that if DCAN is detected early, proper treatments can be performed so that further deterioration of nerves can be either minimized or reversed (1). Thus, an early and sensitive diagnosis of DCAN is critical. In addition, such diagnosis approach should be noninvasive and convenient to patients, which will facilitate a long term monitoring because the onset of DCAN in diabetic patients is uncertain and highly variable. To this end, our goal of this work is to develop noninvasive computational approaches that can provide an early indication of DCAN which will allow doctors to give patients prompt treatments to either mitigate further deterioration or reverse nerve damage.

To date, noninvasive approaches for accurate and early detection of DCAN have not yet been established. Lacking effective diagnosis of DCAN precludes proper treatment which will ultimately lead to irreversible nerve damage. One of the widely-used noninvasive approaches for assessing DCAN involves the analysis of heart rate variability (HRV) signals. Power spectral density (PSD) of HRV signal has been shown to approximate both sympathetic and parasympathetic dynamics (2). However, this approach has not gained much credence because it cannot separate the parasympathetic and sympathetic activities of the autonomic nervous system, hence, an accurate

assessment of the DCAN cannot be obtained. Further, the PSD largely assumes linear and time-invariant dynamics of HRV signals, which also negatively impact the detection accuracy of DCAN.

To overcome the above mentioned limitations, this work proposes a series of time-varying, nonlinear and non-invasive methods to assess cardiac autonomic dysregulation directly from HRV data. One such non-linear method, which could be easily applied to humans, is based on principal dynamic mode (PDM) analysis of HRV. The PDM method is unique, in that it is able to separate the activities of the parasympathetic and sympathetic systems without pharmacological intervention (3). Further, we have extended the PDM algorithm so that it can track time-varying autonomic nervous system's dynamics. Another technique called modified complex demodulation was employed to investigate time progression of HRV spectrum. This method obtains high time- and frequency resolutions, which facilitate tracking of not only the dynamics of HRV but also, time instant when the ANS activities do occur.

By utilizing these algorithms, we are able to study and analyze a series of both long-term and short-term HRV data. In this study, HRV was acquired from two sources: 1. A telemetry system which provides continuous long-term ECG recordings from conscious 4 month old C57/Bl6 controls and Akita mice, which is a model of insulin-dependent type I diabetes; 2. A mouse tail-cuff pulse oximeter is used to measure Photoplethysmograph (PPG) signal in real time from both conscious 2 - 4 month old C57/Bl6 controls and Akita mice to examine if detection of early onset of DCAN is possible using our data analysis techniques. We performed both immunohistochemistry and Western blot analyses to detect nerve-specific proteins, and compared them against our data analyses techniques.

The main **hypothesis** underlying this work is that the development of diabetic cardiac autonomic neuropathy (DCAN) can be detected and monitored via evaluation of the PDM method which has been shown to provide accurate assessment of the autonomic nervous system's dynamics.

The **specific aims** of this work are summarized as follows:

1) To develop computational methods and apply a non-invasive measurement modality that is suitable for mice applications for calculating cardiac autonomic function. Compare this approach to the traditional HRV analysis methods.

2) To quantify and discern the difference in the autonomic sympathetic and parasympathetic dynamics derived from ECG recordings in 4 month old Akita and age matched C57BL6 mice using computational methods.

3) To compare protein marker expression that is indicative of the sympathetic and parasympathetic nervous systems between Akita and C57BL6 mice. Such comparison is used to support our results from the computational methods.

4) To detect and monitor the progression of DCAN starting from 2 month old to 4 months in Akita mice using PPG as a measurement modality followed by data analysis using the computational methods, and corroborate the results with protein marker for autonomic nerves.

ECG (4 month old mice only) and PPG (from 2-4 month old mice) data were collected via ECG telemetry system and tail-cuff PPG sensor, respectively, to derive HRV signal. We used PDM to separate the sympathetic and parasympathetic dynamics from HRV. To determine protein expression, Tyrosine Hydroxylase (TH) and Choactase (Chat), markers of the sympathetic and parasympathetic nerves, respectively, were evaluated. These protein marker results were compared to the computational approaches performed on HRV data to corroboratetheir accuracy. Furthermore, we examined the data length requirement and the sensitivity of the PDM method. Further,

we applied the PDM to determine if the method is sensitive in detecting the onset of the impairment in the sympathetic and parasympathetic activities in diabetic mice.

BACKGROUND AND SIGNIFICANCE

A. Diabetes mellitus

Diabetes mellitus is a common disease especially in the United States. According to data from the 2011 National Diabetes Fact Sheet, there are 23.6 million children and adults in the United States with diabetes, and over 79 million Americans have prediabetes (early type II diabetes). About one third of them (7 million people) are undiagnosed. The diabetic population with people aged over 20 years is increasing at 1.9 million per year. Diabetes is categorized into either type I or type II. Type I diabetes mellitus is characterized by the loss of the insulin-producing beta cells of the islets of Langerhans in the pancreas, leading to insulin deficiency. This type of diabetes can be further classified as immune-mediated or idiopathic. The majority of type I diabetes is of the immune-mediated nature, where beta cell loss is a T-cell mediated autoimmune attack. Currently there is no cure or prevention for type I diabetes which causes approximately 10% of diabetes mellitus cases in North America and Europe. Type II diabetes is characterized by insulin resistance which is the defective responsiveness of body tissues to insulin. The common outcome of either type I or type II diabetes is the abnormal blood glucose level. It is the complications caused by this abnormal condition that leads to serious health problems.

Patients with diabetes mellitus often suffer from blurred vision, fatigue, and increased urination at the initial stage, and gradually progress into severe complications such as kidney failure, cardiovascular disease and diabetic neuropathy to name a few (4-7). Among all diabetic complications, neuropathy is unfortunately the most severe and pressing problem as the early detection of nerve degeneration is hard to diagnose. Nerve cells and their supporting blood vessel cells are most vulnerable to high blood glucose because none of them are insulin independent for glucose transportation. Excessive internal glucose in the cell results in oxidative stress and cell death. The death of

supporting blood vessel cells also accelerates the death of nerve cells. Consequently, over 60% of diabetes patients are affected by diabetic neuropathy.

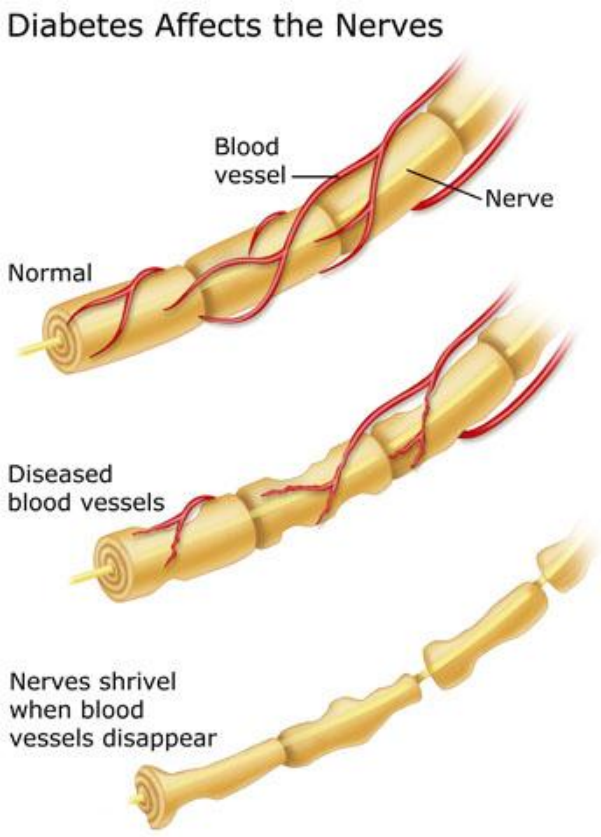

Figure 1. Illustration of nerve and blood vessel cells damaged due to diabetes

B. Diabetic Cardiac Autonomic Neuropathy (DCAN)

The heart is an essential organ that is highly innervated by the autonomic nerves, which are responsible for maintaining cardiovascular homeostasis. A neuropathy in the heart is called DCAN. DCAN is one of the most overlooked of all serious complications of diabetes, and can cause abnormalities in the heart rate control as well as the central and peripheral vascular dynamics (8). Consequences of DCAN include exercise

intolerance, intraoperative cardiovascular lability, orthostatic hypotension, myocardial ischemia, increased risk of mortality, morbidity, and reduced quality of life for people with diabetes. All of these symptoms are manifestations of the autonomic neuropathy (8, 9). As previously described, this complication is currently not curable and not reversible after significant neuronal loss, thus, early diagnosis of DCAN is critical. For human applications, clearly an early diagnosis technique needs to be based on noninvasive measurements, be sensitive, accurate and easy to use. One useful noninvasive method to assess the autonomic function in various physiological and pathophysiological conditions, including evaluation of the autonomic dysfunction in diabetic subjects(10), is via the use of heart rate variability (HRV) time series. It has been shown that the power spectral density calculations of HRV provides an approximation of the sympathetic and parasympathetic (vagal) influences on the modulation of heart rate (11). Interactions between the sympathetic and parasympathetic nervous activities are essential in the regulation of cardiovascular function. The autonomic imbalance, such as sympathetic hyperactivity, promotes life-threatening ventricular tachyarrhythmia, whereas augmented vagal tone exerts a protective and anti-fibrillatory effect (2). Experimental evidence suggests that myocardial ischemia, acute myocardial infarction, sudden cardiac death, and chronic heart failure are associated with some degree of the autonomic imbalance (9). Further, patients who have had a myocardial infarction (MI) have a marked decrease in HRV due to an increase in the sympathetic and a decrease in vagal neural activities (9, 12). Reduced HRV is known to be one of the earliest indicators of DCAN (13) as it has been shown to involve an imbalance of the autonomic nervous system (ANS) (8, 10). A recent study examining the effect of sustained hyperinsulinemic hypoglycemia on the cardiovascular autonomic regulation in type I diabetic and their non-diabetic counterparts has found a reduced cardiac vagal outflow in these patients (10). Another study, examining HRV changes in diabetes, has found that decreases in the

autonomic function is present early in the development of diabetes and that the disease leads to a progressive decline in the autonomic function (14). These above noted findings suggest that HRV can be used as a potential noninvasive indicator of DCAN provided that accurate assessment of the sympathetic and parasympathetic dynamics can be estimated from the HRV signal.

C. Diabetic animal models

Diabetic animal models are used to test the efficacy of our analysis techniques. Further, validation of the computational methods will require animal models since both immunohistochemistry and Western blot analysis necessitate sacrifice of mice hearts.

There have been many different animal models to study DCAN. For example, young adult rats treated with streptozotocin (STZ) developed diabetes with significant reductions in both the heart rate and HRV, suggesting disturbance in the ANS balance (15). In addition, there were significant reductions in the spectral power at higher frequencies, suggesting that the parasympathetic drive to the heart may be altered during the early stages of STZ-induced diabetes (15). Longer duration telemetric recordings used to assess the effect of STZ-induced diabetes demonstrated similar altered autonomic activities (both sympathetic and parasympathetic) commencing at 4 weeks followed by similar continuous depressed autonomic activities even up to duration of 22 weeks (15). Insulin treatment of these STZ-treated diabetic rats showed no significant recovery of the autonomic nervous activity even though heart rate recovered to the pre-STZ treated state (16). This suggests that heart rate itself is not a reliable diagnostic marker of DCAN (6). The literature on diabetic complications subsequently leading to DCAN symptoms in mice is sparse. However, there has been much sophisticated work done on peripheral neuropathy complications using various mouse models (1, 7, 17). An elegant mouse strain without the confounding effects of toxic

chemicals, such as STZ, has been recently introduced and is known as the Tsumuar, Suzuki, Obese Diabetes (TSOD) mouse (type II diabetes). The common traits of these male mice are glucosurea, hyperglycemia, and hyperinsulinemia (18). The TSOD mouse, which is an inbred strain with spontaneous development of diabetes, displays evidence of peripheral neuropathy (18). The mice manifest focal swelling of the myelin sheath in the sciatic nerve, and accumulation of AGE-modified proteins in the endothelial cells of *vasa nervorum*. Furthermore, the nociceptive threshold for pain was significantly lower in TSOD mice (7).

Another intriguing mouse model of Type I diabetes is the Akita mouse. $Ins2^{C96Y}$ Akita mice, which spontaneously develop insulin-dependent diabetes at about 4 weeks of age, express a mutant non-functional insulin isoform (17). Recent studies found that Akita mice exhibit significant increase in fasting blood glucose levels, gait disturbances, and sensory neuropathy (nerve conduction slowing) as early as at 4 months of age (17). To date, research studies detailing the presence and severity of DCAN in Akita mice is scant. Recently, a study using the power spectral analysis has found reduced cardiac efficiency, contractibility and decreased heart rate and heart rate variability in Akita mice, which all imply a possible impairment of the cardiac autonomic regulation (19).

While in the literature the use of STZ is popular, it has many disadvantages. For example, STZ is a toxic chemical which induces diabetes, but it can detrimentally affect and alter many vital organs and can lead to other undesired complications (20). Further, STZ-induced mice do not survive more than 5-6 weeks after the onset of diabetes, thus evaluation of the progression of DCAN is difficult (21). However, Akita mice are known to survive up to 8 months (diabetes onset 3 - 5 weeks of age). In addition, STZ-induced mice and other animal models such as non-obese diabetes (NOD) mice typically exhibit less severe hyperglycemia and less dystrophic neuritis over 4 – 5 months; Akita mice is known to develop peripheral neuropathy at ~ 4 months (17). Mice model such as TSOD

exhibit peripheral neuropathy after 14 months which is also significantly late when compared to Akita mice (20). Further, the control strain of Akita mice – C57BL6 presents very few neuritic dystrophy, thus, Akita mice provide much lower complications than some other strains such as the non-diabetic NOD mice (21). These advantages have led us to use Akita mice as a Type I diabetic model for our studies of DCAN as you can see in Table I.

TABLE I

COMPARISON OF 4 POPULAR MICE MODELS

	Onset of Diabetes	**Life span**	**Severity of Neuropathy**	**others**
Drug Induced (STZ etc.)	After induction	< 5-6 weeks	Less	Highly toxic
Akita	3-5 weeks	8 months	Strong	-
NOD	11-30 weeks	< 5-6 weeks	-	-
Db/db	-	-	Very little	-

Akita is an animal model characterized by spontaneous mutant of the insulin 2 gene such that it produces an improper folding of the insulin and results in the pancreatic beta-cell apoptosis (22). Akita mice start to differ from their control C57BL6 in many physiological and metabolic aspects at a relatively early stage. The parameters reflective of the severity of diabetes in Akita are shown in Table II (17).

TABLE II

ALTERED PHYSIOLOGY PARAMETERS OF AKITA MICE

	WT	B2R-null	BRKO	Akita	B2R-null-Akita	BRKO-Akita
Number of mice	5	5	5	5	5	10
Body weight, g	32.0 ± 1.6	31.1 ± 1.2	37.4 ± 1.6	22.5 ± 1.3*	21.2 ± 1.5*	23.2 ± 1.4*
Kidney weight, mg	245 ± 19	237 ± 35	248 ± 17	239 ± 14	252 ± 10	255 ± 15
KW/BW, ‰	7.80 ± 0.71	7.48 ± 0.89	6.81 ± 0.63	10.67 ± 0.50*	12.21 ± 0.96†	10.91 ± 0.54*
Heart weight, mg	238 ± 22	205 ± 21	184 ± 22	112 ± 4*	110 ± 8*	151 ± 18
HW/BW, ‰	7.50 ± 0.76	6.60 ± 0.61	5.00 ± 0.76	5.75 ± 0.60	5.22 ± 0.17	6.42 ± 0.65
Glucose, mg/dL	142 ± 14	145 ± 9	154 ± 32	798 ± 58*	783 ± 44*	750 ± 32*
Insulin, μmol/L	0.59 ± 0.10	0.95 ± 0.10¶	1.61 ± 0.10‡,§	0.11 ± 0.08*	0.09 ± 0.05*	0.09 ± 0.08*
Urea nitrogen, mg/dL	20.3 ± 1.4	22.1 ± 2.8	22.8 ± 3.0	32.3 ± 4.2	35.6 ± 2.8†	25.8 ± 2.8
Creatitine, mg/dL	0.10 ± 0.03	0.16 ± 0.04	0.12 ± 0.03	0.14 ± 0.03	0.18 ± 0.03	0.13 ± 0.03
Total cholesterol, mg/dL	54.9 ± 9.0	105.9 ± 10.9	85.8 ± 9.0	77.7 ± 7.1	62.9 ± 13.1	67.3 ± 7.6
Triglyceride, mg/dL	55.1 ± 25.1	76.4 ± 14.5	48.1 ± 25.1	105.8 ± 19.8	93.0 ± 27.6	133.8 ± 21.2†
TBARSs, mmol/L	6.5 ± 1.0	17.2 ± 1.6‡	19.0 ± 2.6‡	22.5 ± 1.2*	29.7 ± 2.0¶,*	37.9 ± 2.0‡,§,*
Systolic BP, mmHg	108 ± 3	113 ± 1	114 ± 5	115 ± 2	115 ± 2	115 ± 3

Data are shown as mean ± SEs. WT, wild type; B2R-null, mice lacking B2R; BRKO, mice lacking both B1R and B2R; Akita, mice with heterozygous Akita mutation in Ins2 gene; B2R-null-Akita, B2R-null mice with heterozygous Akita mutation in Ins2 gene; BRKO-Akita, BRKO mice with heterozygous Akita mutation in Ins2 gene; TBARSs, thiobarbituric acid-reactive substances; BP, blood pressure.

*P < 0.01 vs. the nondiabetic group of the same bradykinin receptor genotype;

†P < 0.05 vs. the nondiabetic group of the same bradykinin receptor genotype;

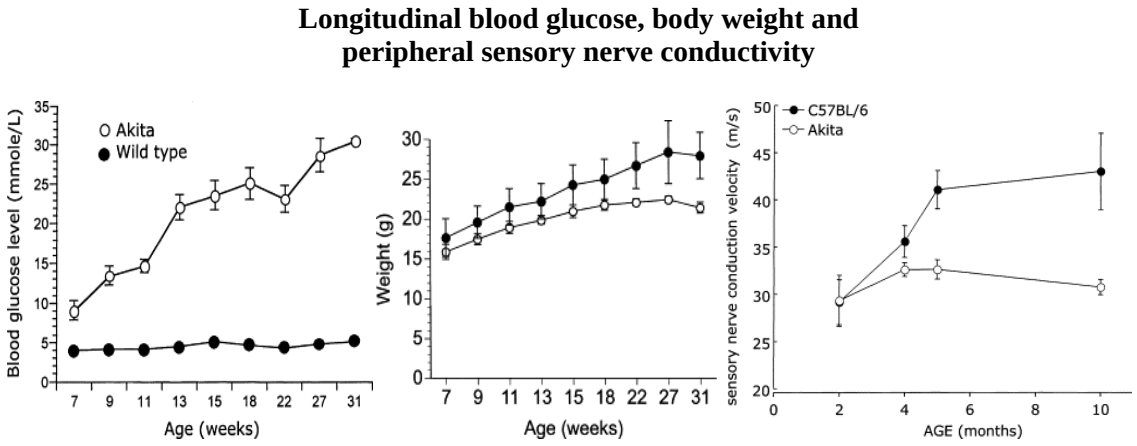

Figure 2. Glucose and body weight change in Akita mice; peripheral sensory nerve conductivity drop noticed at 4 months old

Furthermore, as described above, significant sensory neuropathy (nerve conduction slowing) was found in Akita mice starting at 4 month old, as shown in figure 2 (17). This study did not report the presence of the autonomic neuropathy, however. Thus, it is not clear if DCAN is also present at 4 month old Akita mice. Further, if DCAN is present at 4 months, is it possible that DCAN may appear before 4 months? Thus, two of the main objectives of the present work are to determine the presence of DCAN at 4 month and if it exists, can we reliably detect it even at an earlier stage of the progression of DCAN in Akita mice.

D. Analysis techniques

To date, the power spectral density (PSD) of HRV has been the method of choice as a noninvasive measure of autonomic nervous imbalance in many pathophysiological conditions (2), including diabetes in humans (9, 10, 23) and animal models (15, 24). Specifically, the ratio of the low frequency (LF) (0.04 to 0.15 Hz) to high frequency (HF) (0.15 to 0.5 Hz) power, as obtained from spectral analysis, has been used as a biomarker of the sympathetic-vagal balance in various pathophysiological conditions (25, 26). The LF and HF bands for mice are scaled approximately 8 times higher than those of humans (8) because mice heart rates are ~ 8 time greater than humans. A large LF/HF ratio suggests dominant sympathetic control, whereas a small LF/HF ratio indicates predominant vagal control. However, the utility of the LF/HF ratio for clinical use has not gained a wide acceptance, mainly because it is an approximation of the autonomic balance and does not truly reflect the balance of the two autonomic nervous systems' influences. This shortcoming stems from the fact that the LF/HF ratio assumes that the LF is solely mediated by the sympathetic nervous system, despite the prevailing findings that the LF reflects both the sympathetic and parasympathetic nervous systems (3). Another deficiency of the LF/HF ratio is that the PSD is a linear method, thus, does not

properly account for the nonlinear characteristics of the autonomic nervous system. Many recent studies have shown that the physiological mechanisms responsible for HRV dynamics have significant nonlinear components (2, 23, 27, 28). While the LF/HF ratio obtained via the power spectral density (PSD) is inaccurate, it has paved a way towards developing more accurate non-invasive approaches for determining the dynamics of the ANS.

To overcome the limitations of the PSD, many different computational approaches have been proposed to separate dynamics of the autonomic nervous system (3). Of a noteworthy technique is known as the Principal Dynamic Mode (PDM), as it has been shown to provide accurate separation of the sympathetic and parasympathetic dynamics directly from HRV data (3). The accuracy of the PDM partly is due to the fact that it specifically accounts for nonlinear dynamics of heart rate control, which the PSD does not. The PDM is based on a technique that, among many possible choices of basis functions, it isolates only the minimum number of basis functions that correspond to the essential dynamics of the nonlinear system. Recent studies on human subjects have demonstrated that the nonlinear PDM algorithm is significantly more accurate than the PSD for determining the ANS balance (27, 28). Our results on telemetry recordings of ECG data from Akita mice further demonstrate the accuracy and feasibility of the method in separating the dynamics of the two branches of the ANS without any pharmacological intervention.

E. Nonstationary Power Spectral Density

Analyses of mice HRV, based on time-invariant power spectral densities, do not capture dynamics that change with time. A consequence of this is that subtle changes in dynamics are likely to be missed. To account for nonstationary dynamics in the HRV, we utilize one of the highest possible time- and frequency-resolution spectral methods to

discern and quantify the progression of HRV dynamics during the development of DCAN. The technique is known as the modified complex demodulation method (29). It is a general purpose time-varying spectral method that can be used to understand dynamic characteristics of various biological systems, and offers more accuracy than any other method to date, because it provides one of the highest time and frequency resolutions. The importance of obtaining one of the highest time and frequency resolutions is that it allows us to track not only the transient dynamics inherent in physiological signals at each time instant, but also subtle changes that may occur in the dynamics in response to various stimuli. Note that the time-varying progression of dynamic information is completely lost with the traditional power spectrum, as it is based on a time-invariant assumption. The results section of the Specific Aim 1 briefly highlights the advantages of our time-varying spectral method (29). This time-varying PSD is primarily used as a guide for examining time-varying frequency contents in the LF and HF bands, and is especially appropriate for analyzing long-term telemetry recordings of HRV data. In addition, it is used to verify that the major spectral and time components identified by the proposed nonlinear time-varying PDM method are consistent with the corresponding linear time-varying spectra.

Specific Aim 1: To develop a computational, non-invasive method that is suitable for mice applications for calculating cardiac autonomic function. Compare this approach to the traditional HRV analysis methods.

Heart rate (HR) is predominantly mediated by the autonomic nervous systems – sympathetic system and parasympathetic system; where the sympathetic system elevates heart rate and the parasympathetic system depresses the heart rate. This knowledge has enabled us to study the autonomic function via noninvasive heart rate variability (HRV) analysis.

Traditionally, the power spectral density (PSD) of HRV has been used as a noninvasive measure of autonomic nervous imbalance in many pathophysiological conditions (2), including diabetes in both humans (10) and animal models (15, 24). Specifically, the ratio of the low frequency (LF) (0.04-0.15 Hz for human & 0.4-1 Hz for mice) to high frequency (HF) (0.15-0.5 Hz for human & 1-4 Hz for mice) power obtained from spectral analysis has been used as a biomarker of the sympathetic-vagal balance in assessing HRV (25). A large LF/HF ratio suggests predominantly sympathetic control, whereas a small LF/HF ratio indicates predominantly vagal control. However, the LF/HF ratio for clinical use has not gained wide acceptance, mainly because it is an approximation of the autonomic balance and does not truly reflect the balance of the two nervous influences. This shortcoming stems from the fact that the LF/HF ratio assumes the LF is mediated by the sympathetic nervous system, despite the prevailing understanding that the LF reflects both the sympathetic and parasympathetic nervous systems.

To combat the limitations of traditional approaches, a new nonlinear, time-invariant method that is able to separate the dynamics of the sympathetic and parasympathetic nervous systems has been employed. This new technique, known as the Principal Dynamic Mode (PDM), provides a more in-depth analysis of the ANS and offers a more

accurate measure of the autonomic balance. The method not only specifically accounts for the inherent nonlinear dynamics of heart rate control, but also isolates the sympathetic and parasympathetic innervations. This advantage allows us to examine and describe the true autonomic balance more accurately.

In addition to nonlinearity, most physiological signals' dynamics are nonstationary. As a result, the HRV analysis based on time-invariant power spectral densities (PSD) do not capture dynamics that change with time. This could lead to masking of the differences in the ANS dynamics between DCAN and the healthy conditions. Thus, it is important to have a tool to capture the temporal variation of the ANS dynamics. More importantly, since our telemetry data collection duration lasts a month (24/7), the amount of data collected and to be analyzed is large and certainly daunting. Thus, an effective time-varying method is needed to determine and analyze only those portions of data that are deemed to be stationary. These limitations and demands have motivated us to develop a time-varying method that could account for nonstationary dynamics in ECG data. A technique that can capture nonstationary dynamics is known as the variable complex demodulation method (29). It is a general purpose time-varying spectral method that can be used to understand dynamic characteristics of various biological systems, and it offers more insights than any other method to date, because it provides one of the highest time and frequency resolutions. The importance of obtaining high time and frequency resolution is that it allows us to track not only the transient dynamics inherent in physiological signals at each time instant, but also subtle changes that may occur in the dynamics in response to various stimuli. The results section highlights the advantages of our time-varying spectral method. This time-varying PSD was primarily used as a guide for examining time-varying frequency content in the LF and HF bands and was especially appropriate for long-term telemetry recordings of ECG data.

In this task we developed the advanced analysis technique including the PDM method and nonstationary power spectrum especially suited for mice. These techniques are tested on a short term telemetry ECG testing data to evaluate their performances. They are also compared to traditional "gold standard" time- and frequency-domain methods as they have all been recommended as the standard parameters for evaluating DCAN (2).

Method

HRV Analysis using PDM

In order to separate the activities of sympathetic and parasympathetic systems, we developed a nonlinear method called PDM. The PDM method, originally introduced by Marmarelis, is a method based on extracting only the principal dynamic components of the signal via eigenvalue decomposition (30). The PDMs are calculated using Volterra-Wiener kernels based on expansion of Laguerre polynomials. The application of PDM in HRV analysis was introduced in our previous publication (3) thus were not involved in this paper. Its main idea is described in detail in the following paragraphs. The general input-output relation of a stable nonlinear time-invariant system can be given by the Volterra series as following:

$$y(n) = k_0 + \sum_{m=0}^{M-1} K_1 x(n-m) + \sum_{m_1=0}^{M-1}\sum_{m_2=0}^{M-1} k_2(m_1, m_2)x(n-m_1)x(n-m_2) + \dots$$

where $x(n)$ is the input and $y(n)$ is the output of the system. M is the memory of the system, which is set as 60 in this study. k_i denotes the Volterra kernels, and the quadratic kernel k2 describes the nonlinearity of the system. The estimated output with a maximum lag M can be expressed in a matrix form:

$$y(n) = X^T(n) Q X(n)$$

where T denotes transpose, the vector $X^T(n) = \left[1, x(n), x(n-1), \ldots, x(n-M+1)\right]$ is composed of the input M-point epoch at each time n and a constant 1 that allows incorporation of the lower-order kernel contributions, and Q is a $(M+1)\times(M+1)$ matrix of Volterra kernels with

$$Q = \begin{bmatrix} k_0 & \frac{1}{2}k_1(0) & \frac{1}{2}k_1(1) & & \frac{1}{2}k_1(M-1) \\ \frac{1}{2}k_1(0) & k_2(0,0) & k_2(1,0) & \cdots & k_2(0,M-1) \\ \frac{1}{2}k_1(1) & k_2(0,1) & k_2(1,1) & & k_2(1,M-1) \\ & \vdots & & \ddots & \vdots \\ \frac{1}{2}k_1(M-1) & k_2(M-1,0) & k_2(M-1,1) & \cdots & k_2(M-1,M-1) \end{bmatrix}$$

Then these kernels can be expanded based on L Laguerre functions:

$$y(n) = c_0 + \sum_{j=0}^{L-1} c_1(j) v_j(n) + \sum_{j_1=0}^{L-1}\sum_{j_2=0}^{L-1} c_2(j_1, j_2) v_{j_1}(n) v_{j_2}(n) + \ldots$$

where

$$v(n) = \sum_{m=0}^{M-1} b_j(m) x(n-m)$$

and $[b_j(m)]$ are the Laguerre functions calculated with Laguerre coefficients α=0.5. The number of Laguerre functions L is 8 which is decided by mean-square error criterion. Then Q can be constructed with the estimated kernels (c0, c1, c2) in following way:

$$Q = \begin{bmatrix} c_0 & \frac{1}{2}c_1^T B^T \\ \frac{1}{2}Bc_1 & B^T c_2 B \end{bmatrix}$$

where $B = [b_0^T \; b_1^T \; \ldots \; b_{L-1}^T]$ Laguerre functions are chosen as an appropriate orthonormal basis because they exhibit exponential decaying properties that make them suitable for physiological systems modeling. In addition, due to basis function expansion, the estimation accuracy is maintained even with a small data length.

Since c_2 is a real symmetric square matrix, it can always be decomposed: $c_2 = R^T \Lambda R$ where the eigenvector matrix R is always an orthonormal matrix, and Λ is the diagonal eigenvalue matrix. The second order kernels are solved by $B^T R^T$, and Λ reveals the relative importance of each kernel. We select only the significant kernels based on eigenvalues, as the principal dynamic modes of the system.

The above algorithm theoretically requires white noise as the input to a system. Because only single HR data are available and the real input to a physiological system cannot be as irregular as white noise, a broadband input signal is constructed from the original heart rate series. We first use a time-varying autoregressive model to track the original HR data, then the residual between the estimated signal and original signal is taken as the input of the PDM method. The parameters of the model are estimated by the method of time-varying optimal parameter search (TVOPS) (31), which ensures the performance of tracking. Other tracking techniques also can be used, such as least mean square and time-invariant autoregressive model.

Once the PDMs of HR are obtained from the constructed input, since ANS plays a main role in HR regulation, the two most dominant PDMs in HR usually characterize the dynamics of the parasympathetic and sympathetic nervous regulations respectively. Other eigenvectors are rejected since they may be related to noise or nonessential dynamics. More important, dynamics of sympathetic and parasympathetic systems are separately represented by two dominant PDMs, thus the problem of PSD method is avoided. These two PDMs were converted into frequency domain by FFT to quantify the strength of PDMs by power spectrum. The PDM representing the sympathetic system has its dominant peak in the LF band of HRV, and henceforth it is termed the LF PDM. The PDM of the parasympathetic system contains frequency components from both LF and HF ranges, because the parasympathetic activity within LF range is also captured by this PDM. With its majority power in the HF range, this PDM is termed the HF PDM.

MSE of PDM method using HRV derived from ECG

C57/BL6 **Akita**

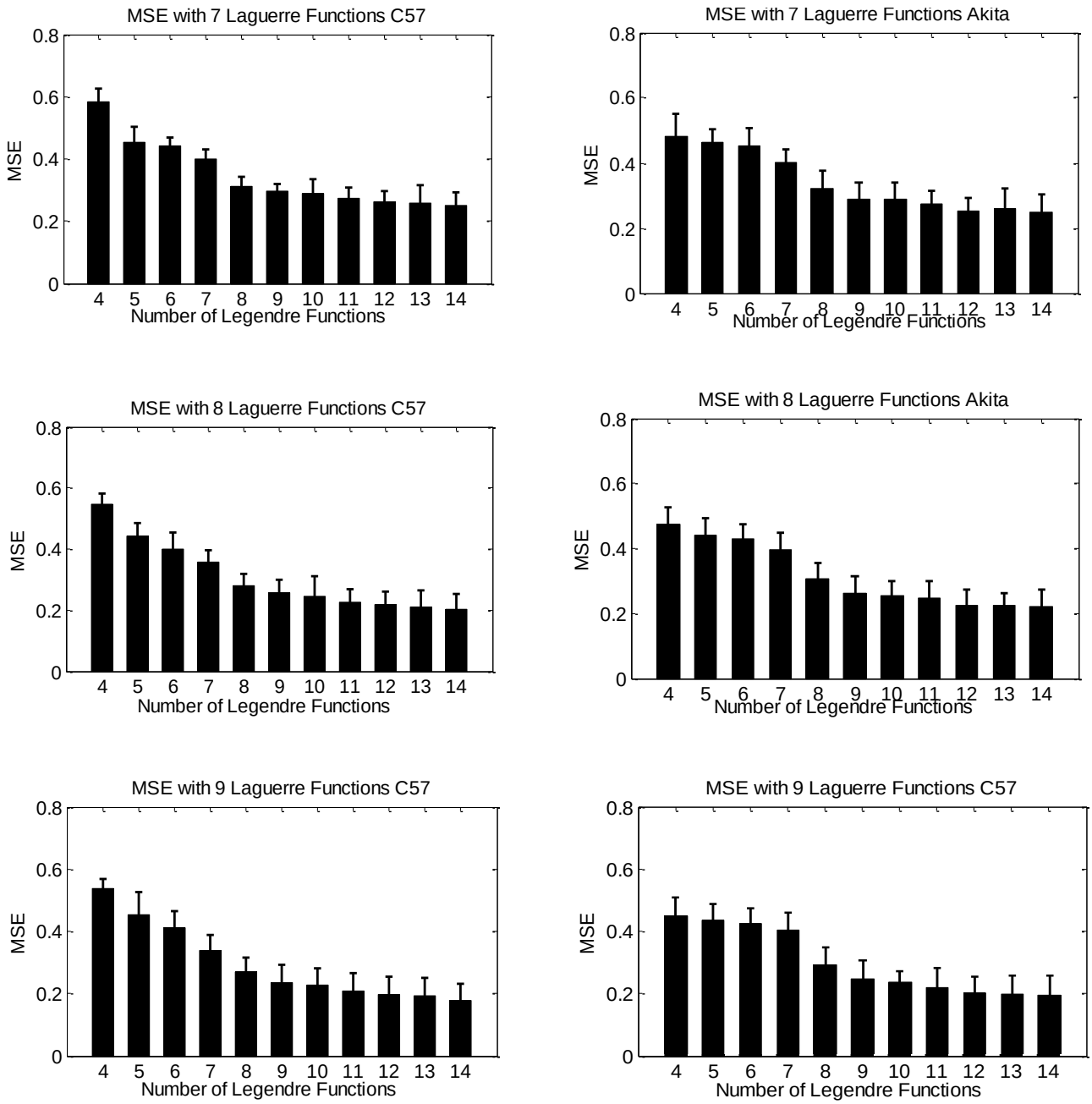

Figure 3 MSE of PDM methods with different number of Laguerre functions and Legendre functions.

Results are based on ECG signal

Hereafter, we also have a LF/HF ratio of PDM to reveal the balance between two nervous systems.

The number of Laguerre basis functions, L, determines the accuracy of the estimated Volterra kernels but care should be used not to over fit by using a large L. The memory length, M, should be set to be long enough to characterize the complete dynamics of the system. The determination of the number of time varying basis functions (Legendre function), W, requires some *a priori* knowledge of the nonstationarities in a system. In general, a larger W is needed to track faster nonstationary dynamics. We have based our choice of the appropriate values of L and W on the mean-square error criterion. The different combination of Legendre and Laguerre function is presented in figure 3. We have systematically determined the minimum data record length needed to obtain reliable estimates. Sixty seconds of data recording is used and this data length is determined by the PDM requirement. This initial minimum amount of data is needed for the method to learn and minimize errors to insure accurate tracking of time-variant dynamics.

Nonstationary Power Spectral Density

Analyses of mice ECG data, based on time-invariant power spectral densities, do not capture dynamics that change with time. A consequence of this is that subtle changes in dynamics are likely to be missed. To account for nonstationary dynamics in the ECG data, we have utilized one of the highest possible time- and frequency-resolution spectral methods to discern and quantify the progression of HRV dynamics during the development of DCAN. The technique is known as variable frequency complex demodulation (VFCDM), which was recently developed (29). The details of VFCDM method is well documented in (29), thus, are not included here.

Thirty minutes of HRV data segments from both Akita and C57/BL6 were used to test the VFCDM method as well as PDM method. HRV was calculated from short term ECG and each data segment was zero-meaned, and detrended. Since animals present different ANS activities in resting state versus active state, we also selected day time segment and night time segment from both strain to compare the ANS function under different states.

Results

A. Comparison of PDM Analysis to Traditional Method.

We tested the ability of PDM to separate the dynamics of the autonomic nervous system on 24-hour telemetric recordings of mice heart rate data. The ECG data were collected continuously 24 hours per day for 5 days. Data recording commenced 1 week after the transmitter device was surgically implanted in sex- and age-matched mice: two C57/B16 control mouse and two Akita mice. For the results presented, we chose arbitrary 5 h segments representing day and night on the 5th day of the 24 h ECG data recordings. The daytime recording was the segment from 11 AM to 4 PM and the nighttime recording was 11 PM to 4 AM. Each of these 5 h recordings was further segmented into 5 min intervals (thus, 60 intervals). The 60 intervals were averaged day- and night-time segments.

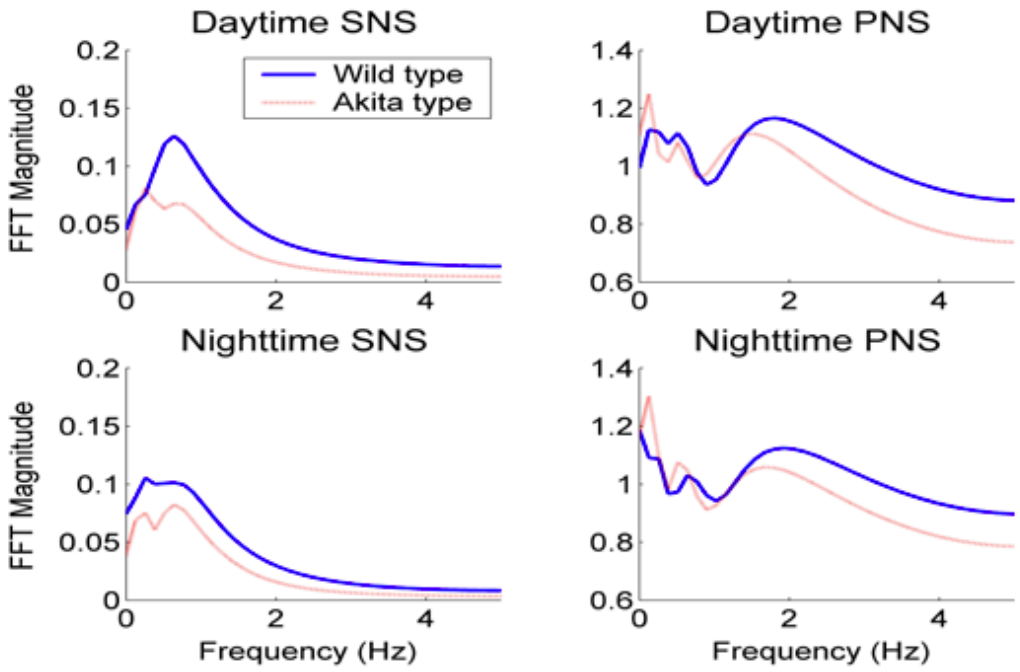

Figure 4. PDMs representing frequency characteristics of the sympathetic (left panels) and parasympathetic (right panels) activities during day (top panels) and night (bottom panels). Note that the parasympathetic nervous system's (PNS) dynamic contains significant spectral power in the low frequencies as well as high frequencies whereas the sympathetic nervous system (SNS) power is contained only in the low frequency ranges.

The PDM methodology provides two PDM spectra that correspond to the main frequency-response characteristics of the two branches of the ANS: sympathetic and parasympathetic. The top and bottom panels of figure 4 show frequency responses of the two PDMs for the Akita and wild type mouse obtained during day and nighttime, respectively; they correspond to the dynamics of the sympathetic (left panels) and parasympathetic (right panels) nervous activities. The top left panel has a dominant peak centered at ~0.07 Hz, which is in the typical frequency range of the sympathetic nervous system. The second PDM (Figure 4: right panels) shows a prominent peak centered at ~0.07 Hz as well as a secondary peak at 2 Hz. The significance of these two peaks in the right panels is that our method correctly identifies the low and high frequency bands that the parasympathetic nervous system is known to operate in. Hence, the PDM method

allows separation of the two nervous activities that are known to interact nonlinearly. More importantly, for both night and day, there are significant reductions in the PDM magnitudes associated with parasympathetic and sympathetic nervous activities in the Akita mouse (red lines) as compared to the wild type mouse (blue lines). In addition, the standard deviation of normal-to-normal (SDNN) beats was markedly reduced in the Akita mouse compared to the wild-type mouse. A similar reduction in sympathetic amplitudes and reduction in SDNN has also been observed with STZ-treated rats (16, 24, 32, 33).

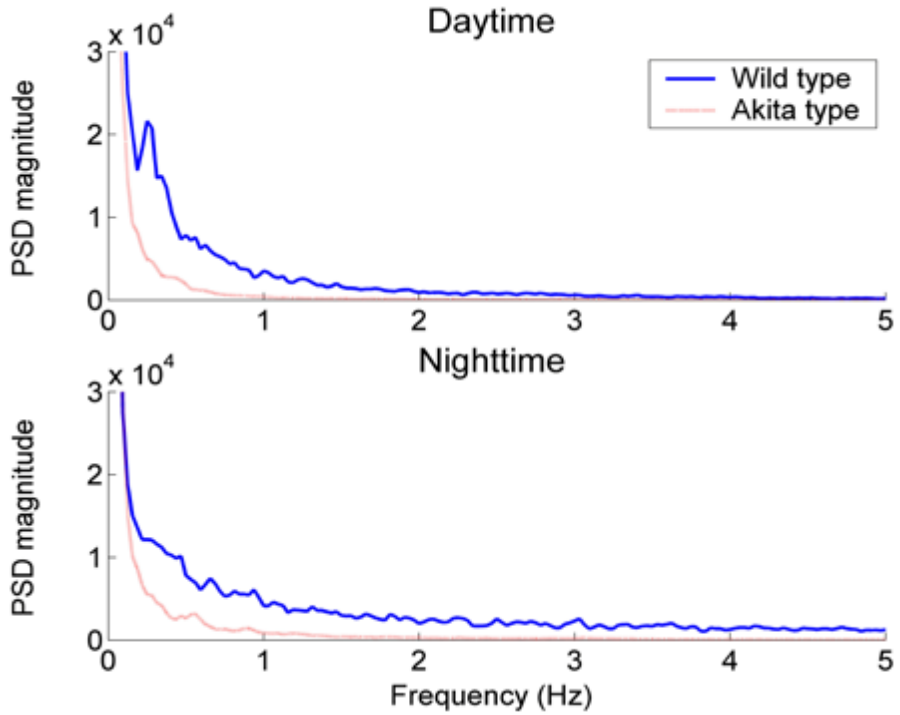

Figure 5. PSD representing frequency characteristics of the sympathetic and parasympathetic activities during day (top panel) and night (bottom panel) recordings. Note that the low frequency (0.4-1 Hz) regime has the activities of both nervous systems, hence, separation of autonomic dynamics is not possible with the PSD method.

For comparison, power spectral density (PSD) results from the same wild type and Akita mouse are shown in figure 5. Similar to the PDM results, a significant reduction in

the spectral power in the Akita mouse is observed for both day- and night-time recordings. However, it is unclear whether the low frequency spectral power reduction is due to a decrease in the sympathetic or parasympathetic nervous activities since the low frequencies (< 0.1 Hz) are attributed to actions of both nervous system activities.

To examine the effect of sympathetic and parasympathetic dynamics on heart rate regulation in short term (over 7 days) in a representative Akita mouse, we show in figure 6, comparison of both the power spectral density and our PDM method. The top panel shows heart rate data and the middle panels show both low frequency and high frequency power estimated by the power spectral method, respectively. The bottom panel shows the separated sympathetic and parasympathetic magnitude using the PDM method. Each data point in all panels represents an average of 420 minute data segments (~7 hours) obtained during animal's day time (sleeping or quiet state) recordings. As previously described, the power spectrum is not able to separate the dynamics of the autonomic nervous system, and it is assumed that the LF and HF are predominately mediated by the sympathetic and parasympathetic nervous activities, respectively. The power spectral results do not correspond well with the heart rate data shown in the top panel. For example, for the first 3 days, the LF increases while the HF decreases which, in combination, should result in a higher heart rate, but the opposite is seen with the heart rate data shown in the top panel. Similarly, from day 4-6, there is increase in HF and a relatively constant LF power, which should result in a net decrease in heart rate, but as the top panel shows, we see a small increase in the heart rate. The PDM method, shown in the bottom panel, corresponds well with the heart rate data shown in the top panel. First, note the greater parasympathetic PDM than the sympathetic magnitude as the data were based on day-time recordings (animal's sleep or resting state). With the PDM method, a decrease in heart rate in the first 3 days can be

explained by the increase in the parasympathetic activities. Furthermore, an increase in the heart rate from days 4-6 can be explained by increase in the sympathetic and decrease in the parasympathetic PDM magnitude. Therefore, these results show that the PDM method is far more physiologically relevant and accurate than the power spectral density approach.

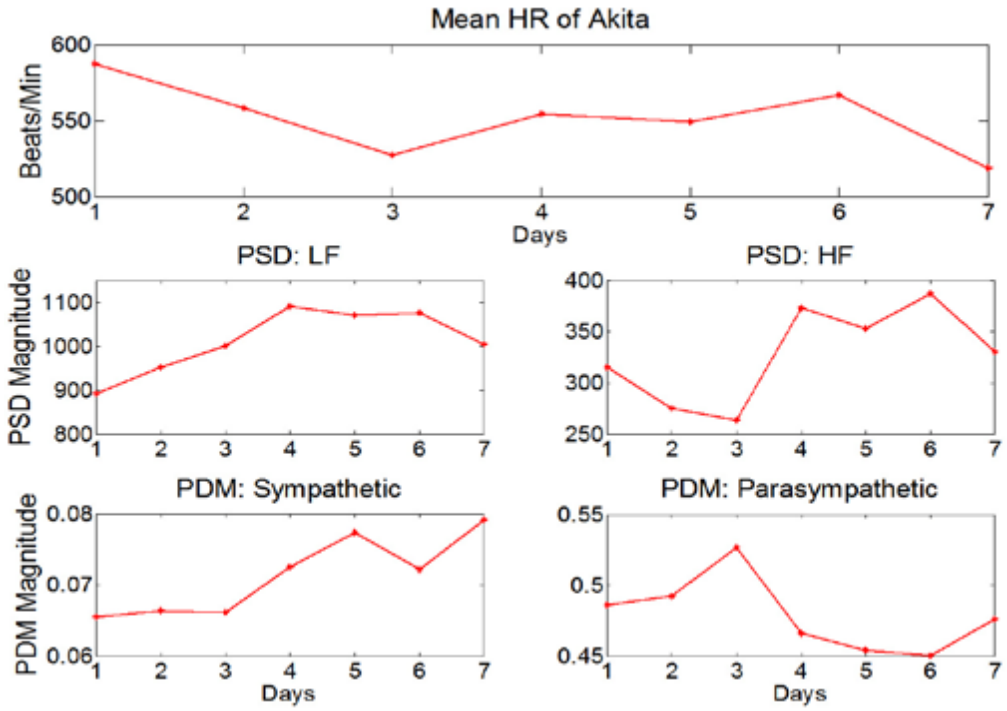

Figure 6. PDM analysis of autonomic balance in a diabetic Akita mouse. HR was measured via telemetry.

B. Time varying power spectral density

An underlying assumption in the traditional power spectrum method is signal stationarity, i.e., that the frequency components of the signal do not vary with time. As most biological signals are time-varying on some scale, the traditional time-invariant power spectrum is not generally an appropriate approach in the analysis of ECG signals, which do have transient components. For example, suppose you have a signal that represents the vertical motion of a point on the wheel of a car over the course of a journey. Its frequency of motion would vary depending on whether the car is moving at

constant speed, accelerating, decelerating, or at rest. Analysis of this record with traditional time-invariant PSD methods would only show the range of frequencies of motion achieved over the course of the entire journey, but it fails to provide information about the time order in which they occurred.

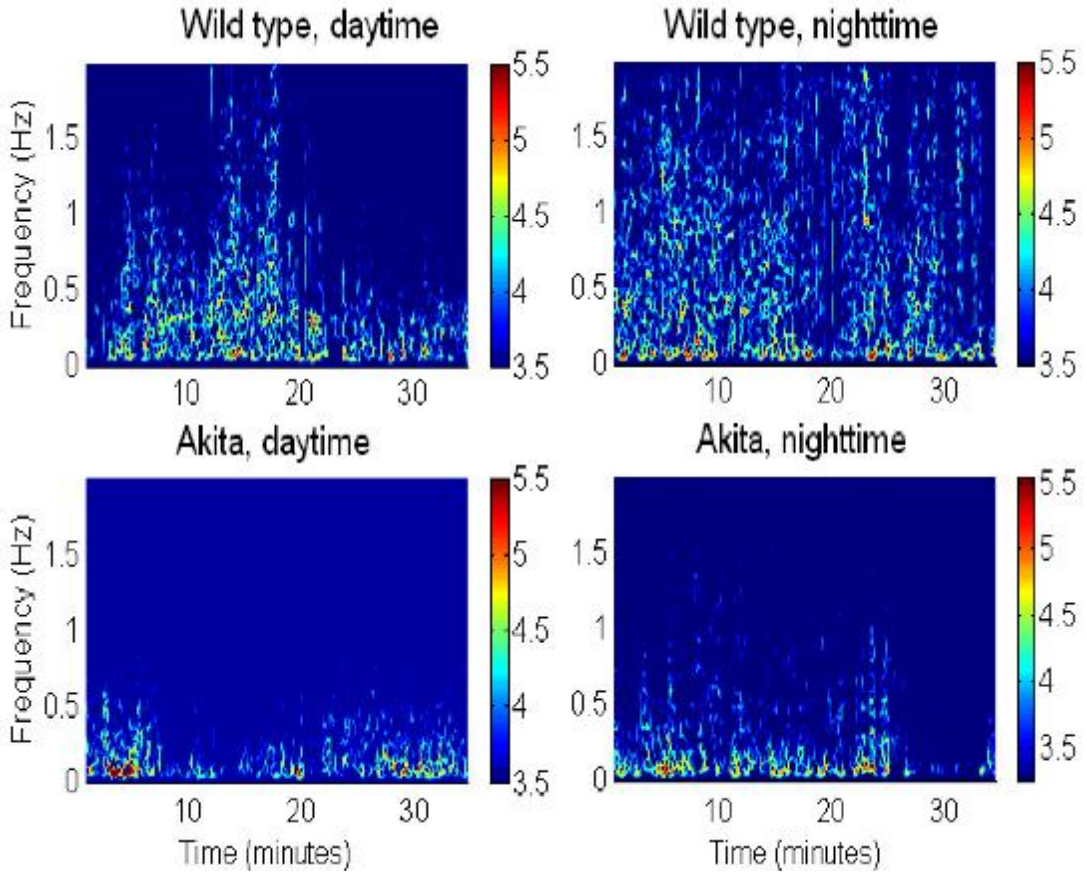

Figure 7. Time-frequency spectra of a wild type (top panels) and an Akita mouse for ~30 min HRV recordings from day (left panels) and night (right panels) settings. Note that mice are more active at night.

To overcome this limitation, we applied a high-resolution approach to estimating time-frequency spectra and associated amplitudes and it is termed the time-varying optimal parameter search-variable frequency complex demodulation (TVOPS-VFCDM) method. Application of the TVOPS-VFCDM time-frequency spectral method to both wild type and Akita mouse HRV data (~30 min of recordings during daytime and nighttime) is shown in figure 7. There is clearly a greater presence of parasympathetic and

sympathetic activities in the wild type than Akita mouse and this difference becomes even more pronounced during nighttime. The striking difference that is clearly discernable is the lack of high frequency power with the Akita mouse during both night and daytime when compared to a wild type mouse. Statistical quantification of these time-varying spectral powers can be done using our method. Further, note the transient dynamic characteristics of the parasympathetic and sympathetic nervous activities, as the frequencies corresponding to them are not constant for all time scales. As a result, we cannot neglect the nonstationarity when averaging sympathetic or parasympathetic activities, which should be especially concerned when we make comparison between Akita and wildtype in the following specific aims.

Summary

In this specific aim, we applied a nonlinear PDM method that could uniquely separate autonomic functions and a high resolution time-varying spectrum to analyze the nonstationarity in the HRV. We compared our PDM method to traditional PSD method in quantifying autonomic dynamics and we can conclude that our developed nonlinear PDM method is able to successfully capture mice's cardiac regulation of ANS system. In figure 4, we observed that the PDM method extracted two dynamics from HRV, named SNS and PNS, had different frequency spectral characteristics. During daytime, the detected sympathetic was elevated while parasympathetic was suppressed compare to nighttime, which corresponds to the fact that sympathetic activity decreases and parasympathetic increases under sleeping condition, and vice versa for day time. This result is similar to some observations using traditional time- and frequency approaches (26, 34). However, as we mentioned above, traditional frequency method is not accurate enough to quantify sympathetic and parasympathetic activities due to the

finding that the former contains only LF components but the latter contains both LF and HF components. Note that from figure 4, the parasympathetic activity extracted using PDM had a peak power in both LF and HF band, which correctly characterizes the parasympathetic dynamics. Meanwhile, the sympathetic dynamics only presents in the LF band. Hence this method allows us to accurately describe autonomic balance calculations. With this advantage, we can now better quantify individual ANS activities and study the impairment of and imbalance of ANS regulations in the following specific aims.

We also tested mice HRV using nonstationary power spectral density-VFCDM, and significant nonstationarity was found in all cases. The results indicated that same animal has different HRV spectral characteristics in different states (defined as daytime and nighttime here); moreover, even at the same state (daytime or nighttime), the nonstationarity was still not negligible. This might be due to the fact that when animals are at different activity conditions (for example: playing vs. resting), autonomic function is certainly altered. If we made a comparison between animals under different states or different activity condition, the interpretation would be skewed (in top-left panel of figure 7 for instance, the first 10 minutes of Akita had stronger LF power than last 10 minutes of WT during daytime). This nonstationary phenomenon implied that in order to accurately describe autonomic function as well as to make an unbiased comparison between Akita and wildtype, an appropriate data processing strategy is necessary to eliminate the time-varying influence.

Specific Aim 2: To quantify and discern the difference in the autonomic sympathetic and parasympathetic dynamics between Akita and C57BL6 mice based on ECG using developed computational, non-invasive method.

It has been found that peripheral neuropathy occurs in Akita mice as early as at the age of 4 month old, however, there have been no studies reporting the presence of the autonomic neuropathy in this mice model. As we expect the autonomic neuropathy to happen no later than peripheral neuropathy, we are interested in examining whether or not DCAN is present in the 4 month old Akita mice using the PDM method.

The PDM is a computational method which could be applied on HRV series calculated from ECG. We use a telemetry system which records mice ECG via an implanted ECG probe. This system enables us to acquire high quality ECG signal and perform HRV analysis to evaluate the autonomic function. Although the telemetry system is invasive largely to prevent mice from contaminating the sensor, for human use in the future, it will rely on noninvasive measuring methods such as a Holter monitor device. Due to a large size and heavy weight of an ECG sensor, we have studied only the 4 month old mice. Note that the weight of an ECG sensor is ~5 gms while 4 month old Akita mice is on average weights ~25 gms. Thus, using an ECG sensor on mice that are younger than 4 months old mice is not feasible. Also in this study, we were interested in examining if there is any further deterioration of DCAN as Akita mice aged.

As mentioned, the power spectral density (PSD) of HRV has been used as a noninvasive measure of the autonomic nervous imbalance in many pathophysiological conditions (2), including diabetes in humans (10) and animal models (15, 24). Specifically, the ratio of the low frequency (LF) (0.04 to 0.15 Hz) to high frequency (HF) (0.15 to 0.5 Hz) power in human subjects, as obtained from spectral analysis, has been used as a biomarker of the sympathetic-vagal balance in assessing HRV (25). The LF and HF bands for mice are scaled approximately 8 times higher than those of humans (8). A

large LF/HF ratio suggests predominantly sympathetic control, whereas a small LF/HF ratio indicates predominantly vagal control. However, the LF/HF ratio for clinical use has not gained wide acceptance, mainly because it is an approximation of the autonomic balance and does not truly reflect the balance of the two nervous influences.

To combat this limitation, in the previous specific aim we applied an advanced nonlinear PDM method that is suitable for mice HRV analysis, and it showed promising results in ANS quantification of HRV. In this task we used the PDM method to investigate ANS function of Akita mice and compared it to the traditional time- and frequency parameters. The duration of data recording was 1 ~ 2 months of continuous ECG data.

Method

Animal surgery and ECG transmitter implantation

The experiment was performed on 10 age-matched male C57BL/6 (wildtype) and Akita mice at 4 month old. All animal-related experimental protocols were approved by the Institutional Animal Care and Use Committee at Stony Brook University and Worcester Polytechnic Institute. The surgery was conducted in accordance with Division of Laboratory Animal Resources (DLAR). Subjects were first anesthetized in a chamber with isoflurane and maintained anesthesia with 1% isoflurane in 50% oxygen/50% nitrogen on a surgical table. During the whole surgery isoflurane concentration was adjusted within a range of 0.8% to 1.5% to keep animal unconscious and to prevent vital damage to the animal. The wireless ECG transmitter was then embedded subcutaneously in the dorsal part of the animal, and wired electrodes were threaded under skin to reach the position of Einthoven bipolar lead II configuration. To maintain fine continuous signal recording, the electrodes were sutured to the muscular layer of body wall. Animals

were given antibodies immediately after surgery and kept in a warmed cage to recover from anesthesia. Further, the animals were allowed one week recovery before we start recording of ECG signal.

Telemetry ECG data and mice activities data recording

Long term ECG and physiological data collection: Wireless subcutaneous (in the mid dorsal) ECGs from C57/BL6 control and Akita mice were continuously recorded for two months at a sampling rate of 1 KHz via a biotelemetry system (Data Sciences International, St. Paul, MN). We recorded the 'activity' of each animal via an animal activity meter, (Columbus Instruments Inc., Columbus, OH). There are two reasons to record activity data: 1. as mentioned in the last specific aim, animals at different activity level have significantly different ANS activities (i.e. day time vs. night time). 2. During long term recordings, animals are alert thus their movements, body scratching or some other activities could induce noise which can significantly impact the quality of the signal. Activity recordings were used to help us to characterize segments that are recorded during a quiet state so that motion and noise artifacts are minimized. Determination of mice's activity was determined by scanning an infrared beam at 160 Hz. Each sensor beam is spaced every 0.5" (1.27 cm) and total counts of beam interrupted at X, Y and Z axes were recorded.

Data segmentations: Among all these data, we compared the difference between Akita and C57 on a weekly basis for duration of 1 month (4 weeks). For each day, we selected a 15 minutes data segment from animals' sleeping time and averaged the results based on every 1 minute of data analysis. Both heart rate (clean and low) and activity data (segments with no activity) were examined to make sure all data segments selected were during a quiet condition (figure 8). To ascertain that our choice of data segment is representative of all data during quiet state, we also select two other 15 minutes'

segments and analyzed them using the same data analysis protocols. Data were analyzed using Matlab r2010a (The Mathworks, Natick, MA)

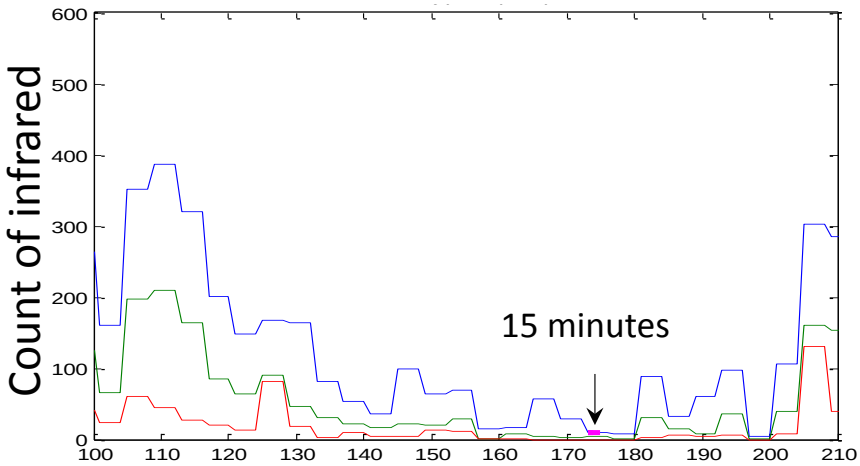

Figure 8 Activity recordings of X,Y, and Z direction, y-axis is the count of object passing a beam

HRV preprocessing

R-R interval series were obtained from ECG using our R-wave detection program. After automatic detection of the R-R series- after removing spikes and premature beats, heart rates were calculated and down sampled to 10 Hz. Note that HRV was equally spaced via the cubic spline procedure as shown in figure 9. SDNN and RMSSD were calculated from the detected R-R intervals. Prior to HRV analysis, all data were detrended, zero-meaned and normalized to unit variance.

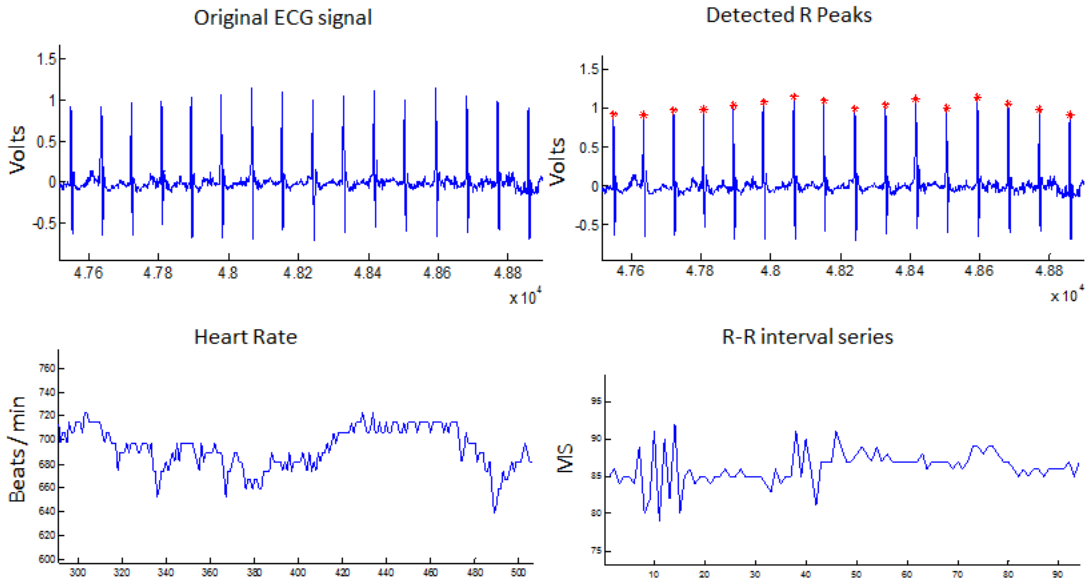

Figure 9 the top left panel presents the original ECG data recorded via Telemetry system; in top right panel, peak detection algorithm was used to detect R peaks in ECG and calculate R-R intervals (bottom right). The R-R intervals are then converted to heart rate (bottom left).

Measurement of time and frequency domain parameters

Time domain parameters including HR (mean heart rate), SDNN (standard deviation of normal-to-normal R-R intervals), and RMSSD (root mean square of successive differences in normal-to-normal R-R intervals), were calculated from the HRV data. The SDNN provides an estimate of overall HRV and the RMSSD yields an estimate of the short term components (HF variation) of HRV. In addition, we computed spectral powers in the low (LF: 0.4-1 Hz) and high frequencies (HF: 1-4 Hz), and the ratio between low and high frequencies (LF/HF) was also calculated. The LF dynamics are believed to represent predominantly the sympathetic activities and the HF represents the parasympathetic tone, whereas the LF/HF ratio reflects the autonomic balance. The Power spectral densities of heart rate data was calculated using the method of the Welch periodogram. We computed the PSD every 1 min to ensure that stationary of the data are

maintained. All of these "gold standard" indices were calculated according to the guidelines of the Task Force of the North American Society of Pacing and Electrophysiology (2). Once we calculate the power spectrum density *LF, HF, LF/HF, we compared them to the performance of these parameters with the PDM method.*

Principle Dynamic Mode

In specific aim 1, the PDM method was applied to short term mice HRV data and the results showed greater sensitivity when compared to PSD approach. The task is to analyze telemetry ECG data using PDM. Same data segments as in previous section were studied. Since PDM requires a broad band input signal, we incorporated TVOPS technique to estimate HRV and use the residual between estimated and HRV data as the input. This residual maintains broad band characteristics and one advantage is that previous heartbeat in one of the factors that influence current heartbeat, thus using this input can better represent the actual system.

Eight Legendre functions were used for TVOPS while 8 Laguerre functions are used for PDM. Out of all available PDMs, we selected only the 2 PDMs that have the greatest significance as they correspond to the sympathetic and parasympathetic characteristics (3). These 2 PDMs were corroborated to correspond to the sympathetic and parasympathetic dynamics as shown in Figure 4. Once these two dynamics are found, we took ratio between the sympathetic and parasympathetic activities to estimate the autonomic balance.

Statistical analysis

For each week, Students t-test was applied to test the difference between Akita and wildtype mice, followed by a normality test of Jarque-Bera test. One-way analysis of variance (ANOVA) with repeated measurement was used to test among each week. Data from three independent data segments were also tested using one-way ANOVA. The null hypothesis is rejected when p-value < 0.05. All statistics were performed using SigmaStat 3.0 (SPSS Inc., Chicago, IL) and Matlab (Mathworks, Natick, MA).

RESULTS

A. Time domain assessment of autonomic function.

We studied 4 month old age-matched male Wildtype (WT or C57) (n=5) and Akita mice (n=5). Four weeks data comparison was presented in figure 10. For each week, data was averaged by taking 15 minutes segment every day. We repeatedly selected 3 different 15 minutes quiet segment according to activity data for every day (represented as in figure 10). We found no significant difference between 3 quiet state segments in all compared parameters, thus we present results from one arbitrary quiet state segment in following figures for simplicity (figure 11 - 13).

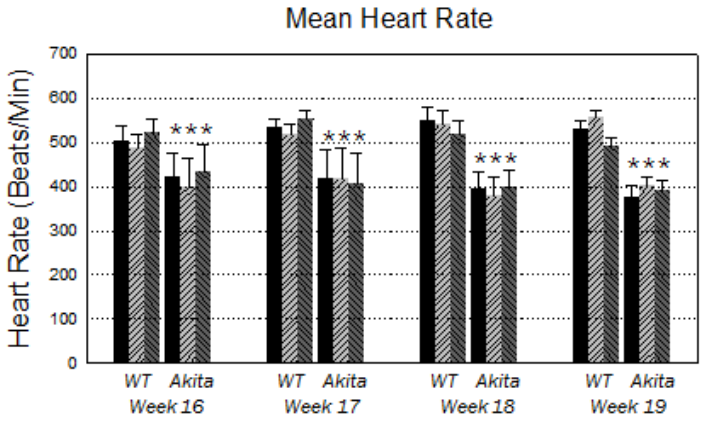

Figure 10. Four weeks mean heart rate comparison between WT (n=5) and Akita mice (n=5). There are three different data segments selected for each week; * denotes statistical significance at P < 0.05

We found consistent and significantly decreased mean heart rate in Akita mice in all four weeks, as shown in figure 11. We also observed reduced SDNN in Akita mice from week 1 to week 4 but a statistically significant decrease was observed in only week 3 and 4. The SDNN parameter is reflective of the overall heart rate variability, thus, a decrease of its value indicated reduced ANS regulation in Akita mice. A time-domain parameter, RMSSD, shows an increase in Akita mice in weeks 3 and 4. The RMSSD reflects parasympathetic dynamics thus our finding via RMSSD parameter suggests that there is higher parasympathetic activities in Akita mice when compared to control mice.

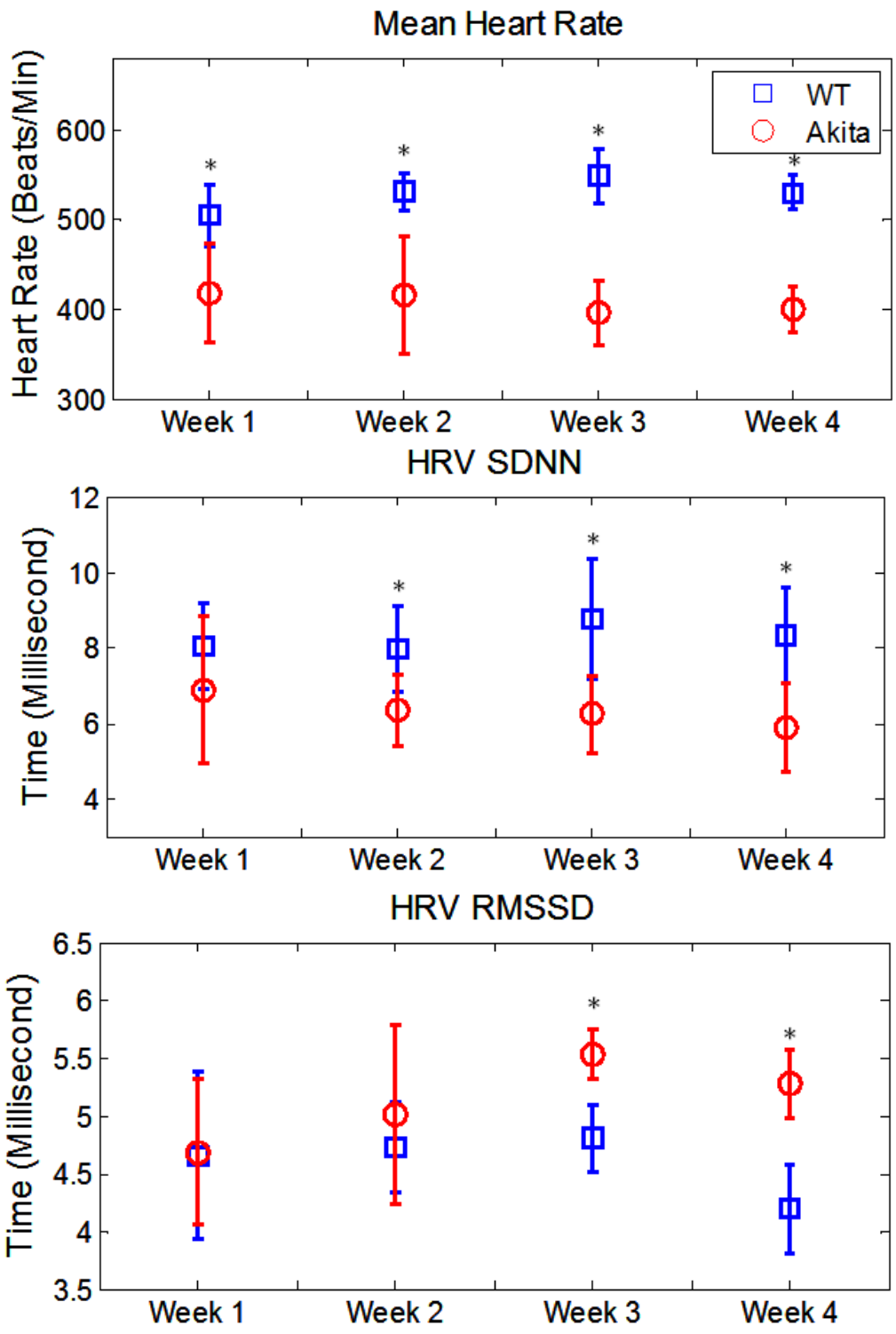

Figure 11, 4 weeks mean heart rate, SDNN, and RSSMD, comparison between WT (n=5) and Akita mice (n=5). There are three different data segments selected for each week; * denotes statistical significance at $P < 0.05$

TABLE III

COMPARISON OF DIFFERENT METHODS FOR HRV ANALYSIS

		Week 1	Week 2	Week 3	Week 4
HR	Wildtype	505 ±35	531 ±21	549 ±31	530 ±19
	Akita	421 ±56 *	417 ±66*	396 ±36*	375 ±26*
SDNN	Wildtype	8.25 ±1.13	7.96 ±1.12	8.78 ±1.61	8.34 ±1.26
	Akita	6.31 ±1.94	6.37 ±0.96	6.26 ±1.01*	5.88 ±1.18*
RMSSD	Wildtype	1.66 ±0.73	1.73 ±0.39	1.81 ±0.29	1.94 ±0.38
	Akita	1.69 ±0.64	2.01 ±0.77	2.24 ±0.21*	2.28 ±0.30*
PSD LF	Wildtype	3.48 ±0.18	3.61 ±0.11	3.62 ±0.21	3.55 ±0.22
	Akita	2.97 ±0.26*	3.07 ±0.40*	2.93 ±0.34*	3.05 ±0.13*
PSD HF	Wildtype	0.73 ±0.14	0.69 ±0.14	0.73 ±0.12	0.76 ±0.08
	Akita	0.77 ±0.08	0.92 ±0.18*	0.99 ±0.09*	0.97 ±0.11*
LF/HF	Wildtype	5.99 ±0.95	6.49 ±0.55	6.74 ±1.35	6.12 ±0.54
	Akita	5.76 ±0.77	5.15 ±2.5	4.43 ±0.80*	4.73 ±0.39*
PDM Symp.	Wildtype	0.86 ±0.04	0.86 ±0.04	0.90 ±0.06	0.88 ±0.03
	Akita	0.76 ±0.06*	0.77 ±0.07*	0.72 ±0.05*	0.72 ±0.06*
PDM Para.	Wildtype	5.04 ±0.49	5.27 ±0.51	5.07 ±0.42	4.89 ±0.35
	Akita	4.26 ±0.34*	4.19 ±0.62*	4.38 ±0.41*	4.27 ±0.30*
Symp. / Para.	Wildtype	0.21 ±0.01	0.22 ±0.03	0.23 ±0.04	0.24 ±0.02
	Akita	0.18 ±0.02*	0.19 ±0.02*	0.19 ±0.01*	0.18 ±0.03*

Mean ± STD, * denotes for statistical significance ($p<0.05$); Akita n=5; WT n=5

B. Frequency domain (spectral analysis) assessment of autonomic function.

As shown in top panel of figure 12, the LF power of Akita mice was observed to be consistently lower than C57 mice throughout the month, which reflects impaired sympathetic innervation. Meanwhile the HF power was significantly higher in Akita mice in week 2, 3 and 4; this result is consistent with lower RMSSD values. This implies greater parasympathetic dynamics in Akita mice. We also estimated the autonomic balance by calculating the ratio between LF and HF. Results shown in figure 13 indicate that Akita mice have a much lower LF/HF ratio in comparison to C57 during weeks 3 and 4. In addition, we observe that there was no difference of these values among all four weeks suggesting that progressive changes in these parameters did not occur.

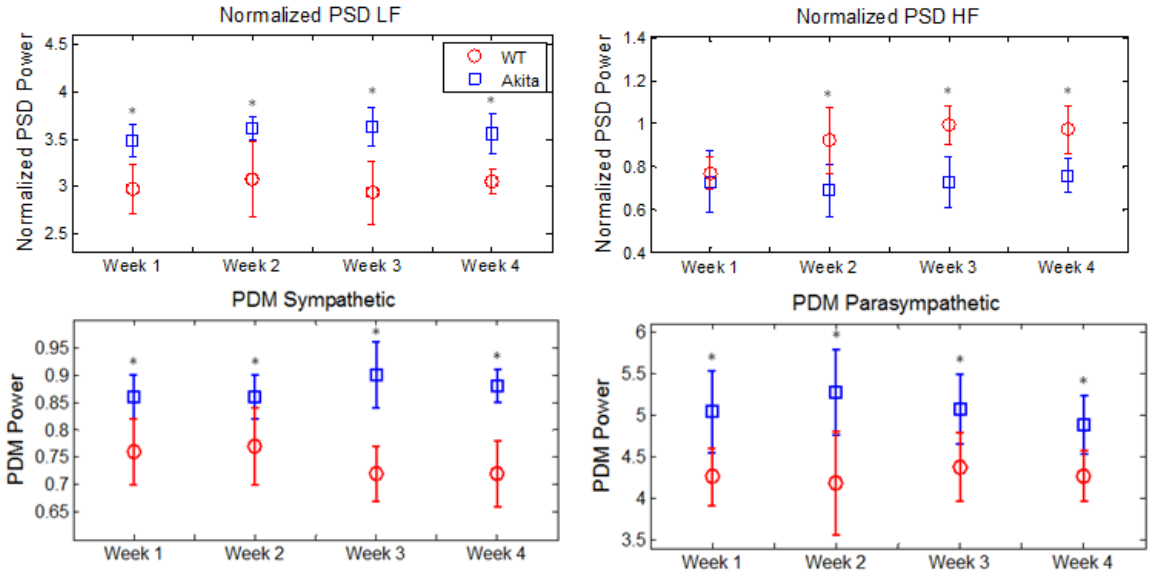

Figure 12. The top panel shows LF and HF power of PSD method; the bottom panel shows the sympathetic and parasympathetic dynamics extracted by PDM method; Akita n=5; WT n=5* denotes statistical significance at $P < 0.05$

C. PDM analysis of sympathetic and parasympathetic activities.

As previously described, the linear frequency domain measures, namely LF, HF band and LF/HF ratio, all fail to represent true dynamics of sympathetic, parasympathetic and autonomic balance due to the fact that parasympathetic dynamics are present in both LF and HF bands. Consequently, we use PDM because it has been shown to separate dynamics of the ANS. As shown in bottom panel of figure 12**,** sympathetic and parasympathetic activities via PDM (from weeks 1 to 4) are found to be significantly reduced in Akita, suggesting depressed or impaired ANS in Akita mice. Note that parasympathetic activities via PDM are lower whereas they were higher with both RMSSD and HF power obtained by PSD. This different result obtained by the two methods for the parasympathetic can only be ascertained by investigating the actual nerves degeneration using gold standard techniques such as immunohistochemistry and western blot analysis (see specific aim 3). Again, the Symp/Parasymp ratio clearly indicates an autonomic imbalance. Further, it was found that there was no difference in our PDM results among all 3 independent data segments suggesting that our choice of a data segment is representative of the overall data. Similar to PSD analysis, we found no progression of DCAN during 4 weeks of recordings.

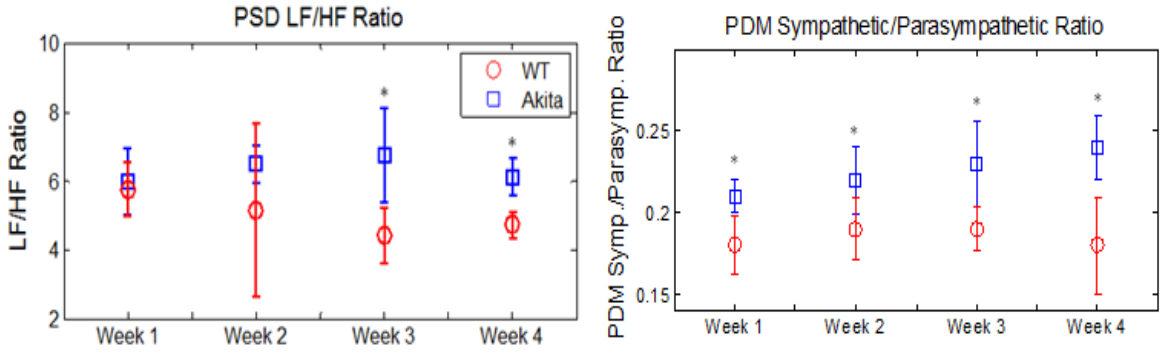

Figure 13. Left panel shows the PSD LF/HF which is the traditional assessment of autonomic balance while the right panel show the autonomic balance estimated via PDM method; Akita n=5; WT n=5;

* denotes statistical significance at $P < 0.05$

Summary

In this specific aim, we have examined the autonomic function via HRV analysis in 4 month old control and diabetic mice. The present results indicate that we were able to detect depressed autonomic function in the type I diabetic mice. First, the mean heart rate in Akita mice was 401±56 beats/min which is almost 20% less than the control wildtype mice (n=5, p<=0.05) at 4 month old. This reduction has been consistent in the following 3 weeks but no further decrease occurred from week 1 to week 4. The time domain parameters, SDNN and RMSSD showed some changes in Akita mice. For instance, the SDNN had a reduced value in Akita mice while RMSSD showed an increased value (only at week 3 and 4). The reduction of SDNN reflects a loss of overall heart rate variability while the increased RMSSD reflects elevated high frequency oscillations. The three frequency domain parameters also showed similar changes in Akita mice where the LF and LF/HF ratio were reduced but HF increased.

The PDM method by its design is expected to provide more accurate results than either the time- or frequency domain counterparts. It was found that there was a reduction in both sympathetic and parasympathetic activities in Akita mice from week 1 through week 4. Specifically, the normalized sympathetic power decreased from 0.86±0.04 to 0.73±0.06 (n=5, P<0.05) while the normalized parasympathetic power decreased from 5.13±0.49 to 4.39±0.34 (n=5, P<0.05) in week one. Consequently, the sympathetic/parasympathetic ratio clearly indicates an autonomic imbalance in Akita mice. Note that both RMSSD and HF PSD showed an increase of parasympathetic activities whereas the parasympathetic PDM showed a decrease. This is certainly a contradictory finding and the ground truth can only be verified by examining the autonomic nerve density as determined by Western blot and immunohistochemistry analysis (see specific aim 3).

So far, we successfully established that our PDM method could not only separate sympathetic and parasympathetic activities from mice HRV but also detect autonomic dysfunction at 4 month old mice. Since our results are all based on computational approaches, it would be important to verify our findings with actual biomarkers of autonomic nerve degeneration in mice heart at 4 months old. Further, another important question that needs to be addressed is how early we can noninvasively detect the autonomic dysfunction.

Specific Aim 3: To validate our results from computational, non-invasive method by comparing protein marker expression that is indicative of the sympathetic and parasympathetic nervous systems between Akita and C57BL6 mice.

Based on the findings in Specific Aim 2, a conclusion can be drawn that Akita mice have autonomic dysfunctions at the age of four month old. Our HRV analysis using PDM approach detected significantly reduced autonomic activity in Akita mice when compared to C57/Bl6 mice. To corroborate our noninvasive PDM finding of the significantly depressed autonomic dynamics, we performed Western blot immunohistochemistry analysis to quantify nerve rarefaction in the SA nodes in both strains of mice, where most of the autonomic nerves are located. Certainly, we expect no autonomic nerve rarefaction in wildtype but expect it in Akita mice. It's well known that nerve cells and the supporting blood vessel cells are most vulnerable to excessive blood sugar concentration (35). As a result, nerve cells die progressively in diabetes and the loss of supporting blood vessels accelerates the process (35). It is reasonable to believe that a reduction of autonomic function observed is caused by the death of the autonomic nerves. The next question is whether or not there is any noticeable nerve density reduction at 4 month old Akita mice. Namely, was the detected autonomic function using our method related to the autonomic nerve rarefaction at SA and AV node where cardiac autonomic innervation occurs? Assuming such a relationship is established, determining how early cardiac autonomic nerve density reduction can be detected becomes extremely important because such a time point can be used as an early diagnosis for DCAN via our noninvasive method. It is due to the limitation of current telemetry technology that we cannot continually record ECG from mice younger than 4 month but better technology

can be expected and eventual facilitate the noninvasive diagnosis at a much earlier time frame.

To achieve the aforementioned goal we need to first corroborate PDM results with nerve density via Western blot in mice heart at 4 month old. Once such a relationship is obtained, we further examine cardiac autonomic nerve density at 2-3 months old mice. Moreover, both protein markers for sympathetic and parasympathetic nerves are tested separately. Immunohistochemistry staining is also employed to visualize overall nerve distribution.

Method

Tissue harvesting and preparation

Three groups of sex- and age-matched (2, 3, and 4 month old) wild-type C57/BL6 (n=5 for each group)and Akita mice were studied (n= 5 for each group).

Tissue Collection Mice were euthanized in a CO_2 chamber. The heart was rapidly excised, and placed into ice-cold phosphate buffered saline (PBS). The atria were separated from the ventricles and washed in clean ice-cold PBS three times each to remove any blood. Any connective tissue attached to the atria was scraped off. The tissue was then moved into a microcentrifuge tube and snap frozen with liquid nitrogen. The tissue was stored at -80°C until use.

Tissue Preparation After thawing of frozen atria tissue on ice, the tissue was placed into RIPA Buffer (1 mL, R0278, Sigma-Aldrich), Protease Inhibitor Cocktail (100 µL, P2714, Sigma-Aldrich), PMSF (10 µL), and Sodium Orthovanadate (20 µL) (total volume of 350 µL was added to each tissue sample). The tissue was diced with a scalpel and kept on ice for 1 hour (periodically vortexed). After the lysis, the sample was centrifuged at 14,000 rpm for 30 minutes at 4°C. The supernatant was then transferred to a new sterile tube and frozen at -80°C until use.

Western Blot Analysis

Western blotting of heart tissue (the atrial section of the heart since autonomic nerves are more prevalent in the SA and AV nodes) (36) was used to quantify levels of proteins of interest in each strain of animals to be utilized. The tissues were homogenized and the proteins fractionated according to size in an SDS-polyacrylamide gel and then transferred onto a membrane for probing with specific antibodies. In this study, we focused on the proteins tyrosine hydroxylase (37)(TH, a marker for sympathetic nerves), synaptophysin (38)(SYN, for general nerves), and choline acetyltransferase (39, 40) (ChAT, a marker for parasympathetic nerves). The amount of protein loaded into each lane was controlled by determining the total protein concentration by running a Bradford Assay for each sample. In addition, the housekeeping protein β-actin was used as an internal control. This ensured that the differences we see within protein abundance (TH, SYN, and ChAT) represent true differences between each study group and not the result of technical artifacts.

SDS Polyacrylamide Gel Electrophoresis 30 μg protein of each sample was diluted with Laemmli Sample Buffer (Bio-Rad) (1:1 dilution), heated at 95°C for 5 minutes, and then centrifuged at 14,000 rpm for 1 minute. The samples were loaded onto a freshly prepared 10% SDS PAGE adjacent to 5μL of a protein ladder standard (PageRuler, Fermentas) and the electrophoresis performed at a constant 115 V (~25 mA) in electrophoresis running buffer (25mM Tris, 192mM Glycine, and 0.1% SDS) until the dye front reaches the bottom of the gel (~1 hour). At this point, the gel was removed from the gel apparatus and rinsed with 1x TBS-T.

Protein Transfer After gel electrophoresis, the proteins was transferred to a PVDF membrane by transverse electrophoresis in a Genie Blotter (Research Products International) as described by manufacturer using 25mM Tris, 192 mM Glycine, and 20%

Methanol as transfer buffer and 100 V for 1 hour at 4°C. After the transfer, the PVDF membrane was removed from the apparatus and washed with 1x TBS-T.

General Immunoblotting Procedure The membrane was first placed into a blocking solution (5% Bio-Rad Blotting Grade Blocker non-fat dry milk, in 1x TBS-T) for 1 hour at room temperature to block non-specific protein binding sites. Next, the membrane was placed in 1% blocking solution containing the primary antibody (at the dilutions given below), overnight, in a cold room. The membrane was then washed 6 times for 15 minutes each with 1x TBS-T. Afterwards, the membrane was placed into 1% blocking solution containing secondary antibody for 1 hour at room temperature, then washed again 6 times for 15 minutes each with 1x TBS-T.

Primary antibodies:

- Tyrosine hydroxylase (TH, for sympathetic nerve): anti-TH, ab112, Abcam Inc. (1:200 dilutions).
- Synaptophysin (SYP, for general nerves): anti-SYP, sc-9116, Santa Cruz Biotechnology, Inc. (1:500 dilution)
- Actin (control): anti-actin, ab50412, Abcam, Inc. (1:5000 dilutions).
- Choactase (for parasympathetic nerve): anti-Choline acetyltransferase, AB144P, Millipore Inc. (1:200 dilution).

Secondary antibodies:

- Anti-rabbit horseradish peroxidase antibody from goat, A6154, Sigma-Aldrich. (1:10,000 dilution).

Membrane Stripping Probed membranes were placed into a stripping buffer (62.5mM Tris-HCL, 2% SDS, and 100mM β-mercaptoethanol) at 50°C for 30 minutes, then washed 6 times for 5 minutes each with 1x TBS-T. The membrane can then be re-probed following the above protocol.

Imaging Chemiluminescence solution (Amersham ECL™ Western Blotting Analysis System, RPN2109, GE Healthcare) was mixed immediately before imaging. The PVDF membrane was soaked in the mixed solution for 1 minute prior to exposure to camera. The image of the membrane was obtained by exposure to Chemi Doc camera for 5 minutes. The ladder image and blotting image was exposed separately and overlaid in Photoshop afterwards.

Immunohistochemistry Analysis

Similar to the Western blot analysis, the immunohistochemistry analysis of autonomic innervation in 4 month old mice heart (near either SA node or AV node) involved the specific nerve markers (Synaptophysin) for general nerves. The heart was snap frozen at -80 C immediately after excised from the animal and sections around SA node area were obtained and fixed on Super Frost Slides. Slides fixed in paraformaldehydewere then stained with aforementioned three proteins as well as a HCN4 antibody (41). The HCN4 is a channel protein only found in SA node therefore it is used as a location control for SA node. Stained cardiac sections were examined on a Zeiss confocal microscope, and the SA and AV node were assessed to quantify sympathetic and parasympathetic innervation. It is well known that SA and AV nodes are densely innervated by the autonomic nerves (36).

Data analysis and Statistical analysis

For each Western blot comparison, the image was inverted and the integrated density of each interested protein band was recorded (using Adobe Photoshop CS4, Adobe). This density value was divided by the integrated density value of Actin in the same well to obtain a normalized value.

Students' t-test was applied to test the normalized integrated density value between Akita and wildtype mice, followed by a normality test of Jarque-Bera test. The null hypothesis is rejected when p-value < 0.05. All statistics were performed using SigmStat 3.0 (SPSS Inc., Chicago, IL) and Matlab (Mathworks, Natick, MA).

Results

A). Western blot assessment of autonomic nerves density.

Our HRV analysis using PDM approach indicates significantly reduced autonomic activity in Akita mice when compared to C57/Bl6 mice at the age of 4 month. To corroborate our noninvasive PDM approach finding of significantly depressed autonomic nervous dynamics, we performed Western blot analysis to quantify nerve rarefaction in the SA and AV nodes in both strains of 4 month old mice (n=5). We expect no autonomic nerve rarefaction in C57 but certainly expect it in Akita mice. As observed in figure 14 all three proteins are less expressed in Akita mice compare to C57, which illustrates a noticeable autonomic nerve (both sympathetic and parasympathetic) rarefaction. We recorded the integrated density of each bar on the Western blot and Actin was used as a control for total protein volume of each lane, thus each calculated density is normalized to the density of actin as the final density. In Table IV, we show the normalized density of each neural marker, which represents a significant reduction of all autonomic nerve in 4 months old Akita. This result corroborates our PDM findings in the previous specific aim.

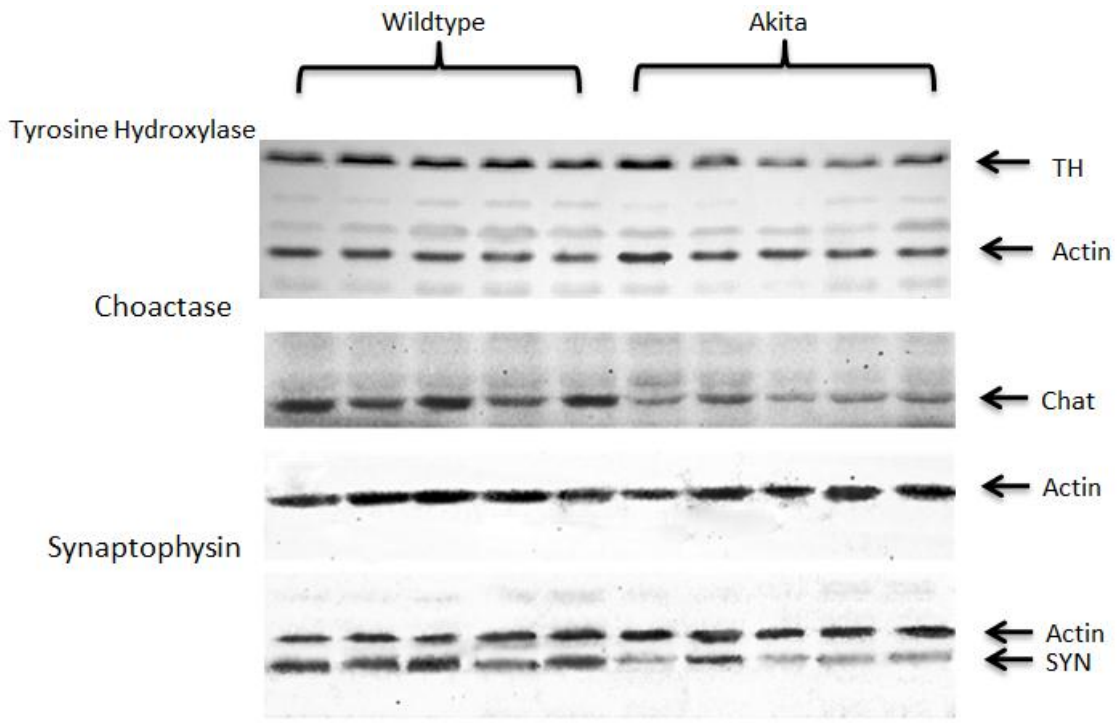

Figure 14, western blot of 4 months old Akita (n=5) VS. Wildtype (n=5), the SYN is a marker for general nerves, Chat marks parasympathetic nerves and TH marks sympathetic

We also investigated the possibility of autonomic nerve rarefaction on younger mice; seeking to potentially diagnose DCAN at an earlier stage using our technique. In figure 15 we show Western blot of TH, SYN, and Chat antibodies in 3 month old mice (Akita n = 5 and wildtype n = 5). After normalizing the integrated density to actin, a significant reduction was found in Akita mice. The same experiments were performed on 2 month old mice (figure 16, Akita n = 5 and wildtype n = 5), however, there was no noticeable reduction. These results indicate an autonomic nerve rarefaction presents as early as 3 month and such a rarefaction might be detected using our approach, as we did in four month old mice.

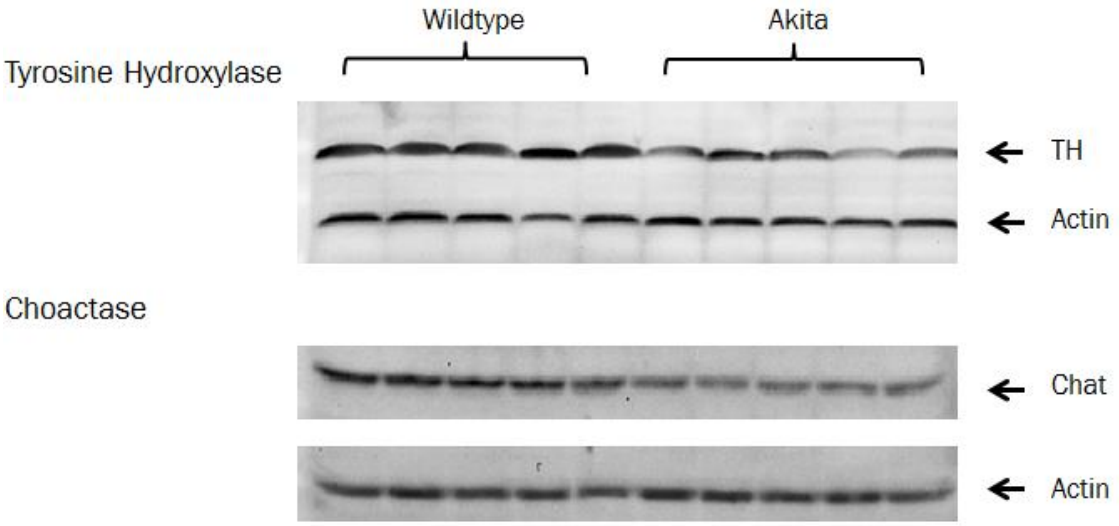

Figure 15, western blot of 3 months old Akita VS. C57, Akita n=5; Wildtype n=5

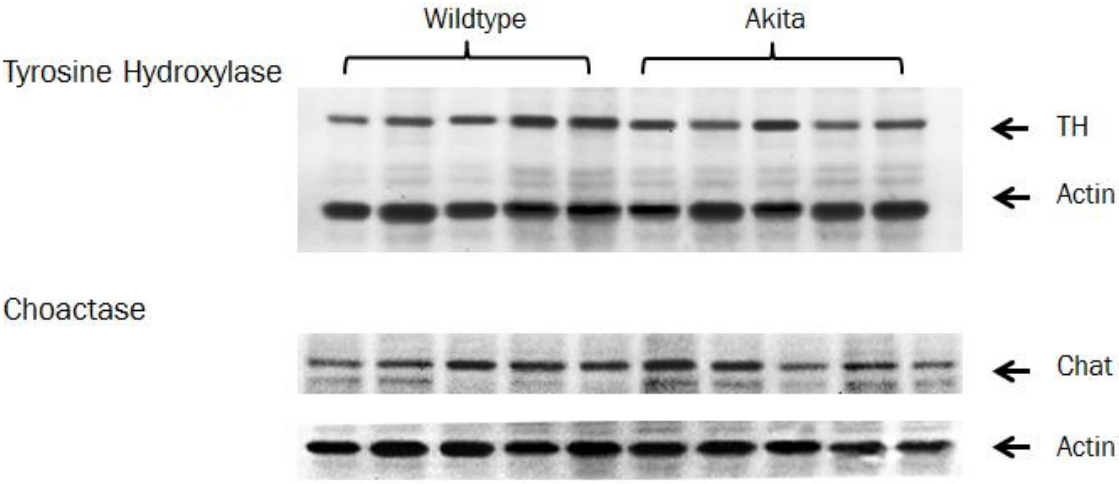

Figure 16, western blot of 2 months old Akita VS. C57, Akita n =5; Wildtype n=5.

TABLE IV

QUANTIFICATION OF WESTERN BLOT ANALYSIS

		TH	Chat	Syn
4 months	WT	1.52 ± 0.18	0.99 ± 0.27	1.14 ± 0.43
	Akita	1.18± 0.20 *	0.66 ± 0.13 *	0.50 ± 0.15 *
3 months	WT	1.11 ± 0.12	1.06 ± 0.07	
	Akita	0.87 ± 0.15 *	0.84 ± 0.02 *	
2 months	WT	0.48 ± 0.08	0.65 ± 0.12	
	Akita	0.49 ± 0.05	0.62 ± 0.07	

The * denotes statistical significance with P <0.05, WT n=5 and Akita =5 for each age group

B). Immunohistochemical assessment of cardiac autonomic innervations.

We also performed immunohistochemical staining on the overall neural markers to examine if indeed total autonomic nerves are less presented in SA node. A general nerve marker (anti-synaptophysin) staining is obtained. Figure 17 shows deconvoluted optical sections double stained for HCN4 (red), a membrane channel found only in sinoatrial (SA) and atrioventricle (AV) nodes in the heart; the synaptophysin (green) was used to stain for general nerves. The negative control was obtained by omitting both primary antibodies and the image was not deconvolved. As shown in figure 17, the SA node in this Akita mouse is clearly less densely innervated than the C57 control; a similar reduction in nerve density was seen in sections of the AV node in this Akita mouse (not shown). This rarefaction corroborates our signal processing results of the reduction of sympathetic and parasympathetic functions.

Comparison of overall nerve density in 4 month old Akita and age matched C57/BL6

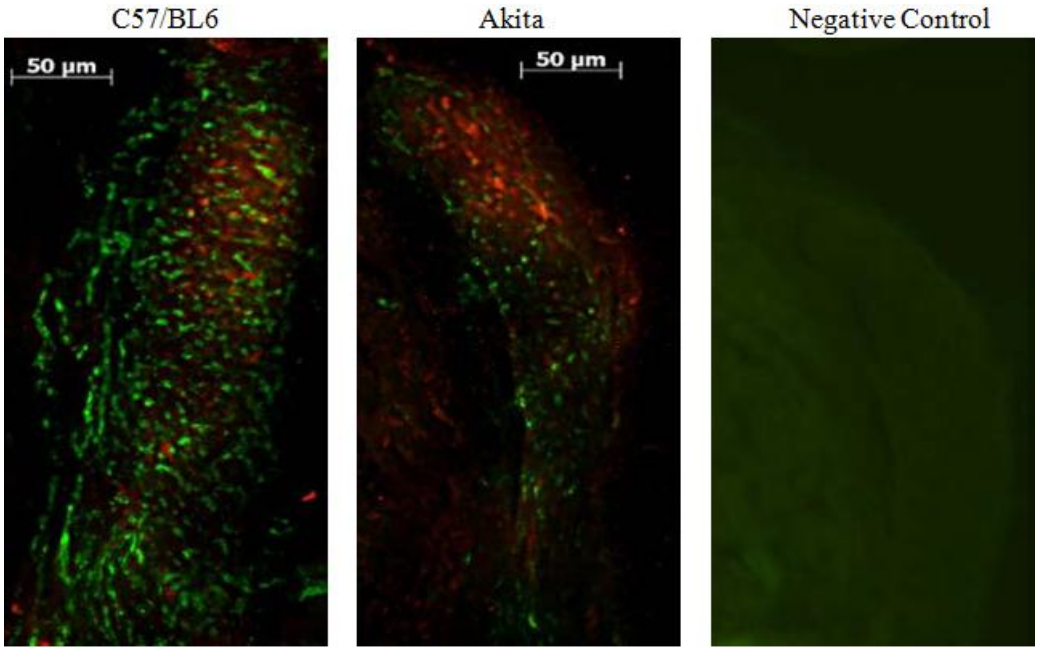

Figure 17, Immunostaining of SA nodes for HCN4 channels (red) and synaptophysin (green). Images are deconvolved optical sections. In the negative control both primary antibodies were omitted, and the image was not deconvolved. The sections were stained concurrently & imaged with the same settings. All the images were cropped and subjected to 20% contrast enhancement.

Summary

In this aim we examined the presence of nerve degeneration using three nerve protein markers: tyrosine hydroxylase (TH, a marker for sympathetic nerves), choline acetyltransferase (ChAT, a marker for parasympathetic nerves) and synaptophysin (SYN, a marker for general nerves). Sex- and age-matched wild-type C57 and Akita mice from 2 month old to 4 month old were compared. In 4 month old Akita, protein markers was found significantly less expressed compared to C57 which corroborated our data analysis findings in autonomic function. This result indicated that the observed autonomic dysfunction at 4 months old is caused by the autonomic nerves rarefaction; in other words, the autonomic rarefaction could be detected using our developed technique in 4 month old Akita. Although we do not have access to 3 month old mice ECG data, a similar reduction of autonomic nerve density was found in 3 month old Akita heart which implied that our method had a potential to diagnose the ANS impairment at that time point. This needs to be further tested in the future.

Finally, there was no nerve degeneration observed in 2 month old Akita and this is similar to other studies on peripheral neuropathy (21). Note that if ECG can be acquired in younger mice, noninvasive HRV analysis can be performed to see if there is a sign of autonomic dysfunction before a detectable nerve degeneration occurs.

Specific Aim 4: To detect and monitor the progression of DCAN in Akita mice based on PPG using our computational, non-invasive method.

In order to detect and monitor the development of DCAN using our computational method, HRV data prior to the onset of DCAN is required. Data analyses in the Specific Aim 2 were performed on HRV series extracted from ECG data on mice that were 4 month old. In this aim, we are interested in examining the onset and progression of DCAN, thus, requiring us to examine mice that are as young as 2 month old. However, due to Akita's small weight and a large size of an ECG telemetry sensor, we chose a pulse oximeter sensor to collect HRV data. It has been shown that heart rate variability can be effectively measured by pulse oximetry (42). The pulse oximeter measures photoplethysmograph (PPG), which reflects the changes in blood oxygenation. Blood and tissue have different absorbance to infrared light, thus, each volume change caused by heart beat is captured by an infrared receptor (43). Although the PPG reflects influences from both heart beat and blood vessel capacity, extensive HRV analysis were performed using PPG and it has shown a good correlation to HRV (44).

One advantage of PPG sensors is that it can be easily attached to animal tails, which in turn does not create physiological stress when compared to an implantable ECG sensor. For our work, we used a commercially-available mice tail PPG system – MouseStat (Kent Scientific Corp.) which allowed us to conduct HRV studies on mice less than 4 months old. Data from 10 Sex- and Age- matched mice (Akita n = 5 and Wildtype n = 5) were recorded starting from 1.5 month to 4 month old. These data were investigated and compared to our previous ECG-based HRV analysis results (when the animal reached 4 months).

Method

Data acquisition

Mice were conscious and restrained in a tube-shaped mouse restrainer with their tails exposed. They are then placed on a heating pad and temperature was adjusted as needed. The Y-clip PPG sensor is placed on the proximal portion of the tail where appropriate humidity is maintained to produce the best signal. Ten minutes settling time was allowed so that a mouse can get used to the restrainer and Y-clip prior to the start of data recording. PPG Data from 10 Sex- and Age- matched mice (Akita n = 5 and Wildtype n = 5) were collected for 30 min. ~ 1 hr. each day, 5 days a week. The entire recording process lasted 2.5 months (1.5 month old mice to when they reached 4 months). PPG data were recorded at a sampling rate of 600 Hz.

Data processing and analysis

For each day, a 15 minute data segment that was free from motion and noise artifacts were selected and averaged based on every 1 minute of data analysis of the entire 15 minutes segment. (note that mice were conscious, thus a large part of data would be corrupted by motion artifacts). In time domain, to obtain heart beat interval, we develop a peak detection program which detected each peak of the PPG wave as shown in figure 18. The time interval durations were recorded as R-R interval series. The SDNN and RMSSD parameters were calculated from the R-R interval series.

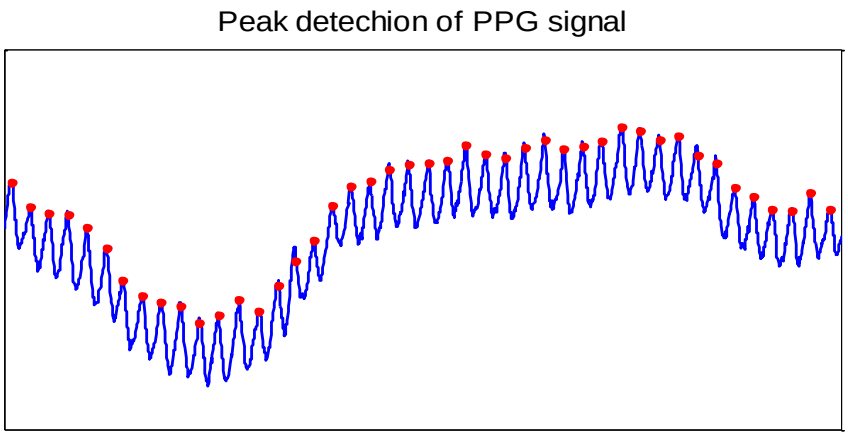

Figure 18, example of peak detection for PPG signal recording

In frequency domain, we obtained HRV by converting R-R intervals into beats/min and using a cubic splining technique to ensure equal sampling of the HRV data. The HRV data were zero-meaned, detrended and down sampled to 10 Hz prior to calculations of the PSD and PDM analyses. The number of basis functions for PDM was determined by the mean square error (MSE) criteria. The MSE values corresponding to different basis function combinations are presented in figure 19. As shown, 11 Legendre functions with 8 Laguerre functions were chosen for our analysis since this combination provided the smallest MSE value. Statistical analysis was performed similar to Specific Aim 2

MSE of PDM method using HRV derived from PPG

C57/BL6 **Akita**

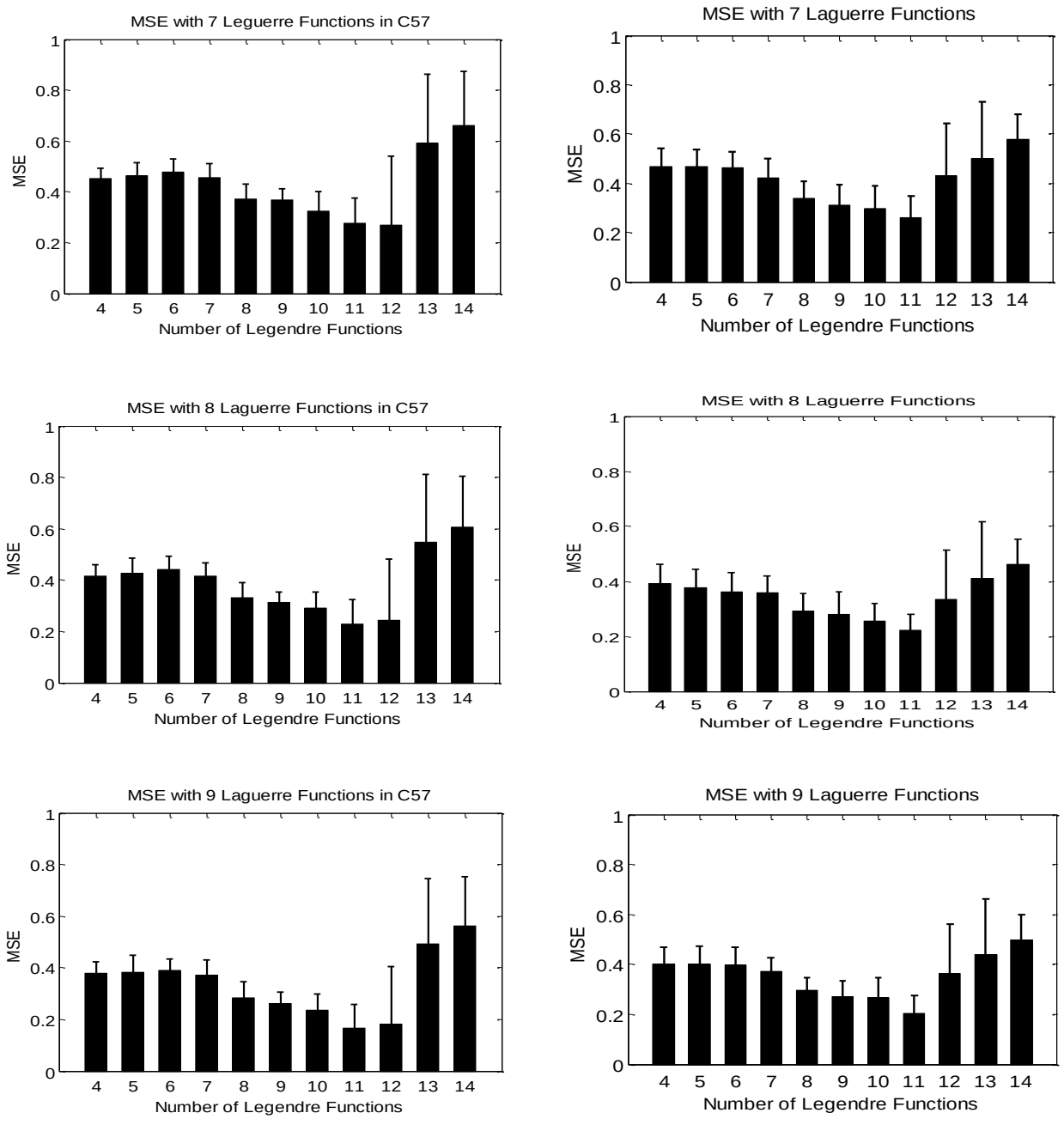

Figure 19, MSE of PDM method with different number of Laguerre functions and Legendre functions.

Results are based on PPG signal

Results

Based on HRV calculated from PPG, we examined the autonomic function via PDM method and the traditional time- and frequency parameters. The PDM results and time- and frequency-domain parameters were compared to previous results obtained from ECG when appropriate (e.g. at 4 months).

A. Time- and frequency- domain assessment of autonomic function.

Similar to the Specific Aim 2, the standard time- and frequency-parameters were investigated on a weekly basis. Results were recorded from week 6 through week 19, thus, 14 weeks of data comparison is presented in figure 20. Each data point is the average of each week, which consists of 15 minutes a day 5 days a week. We have found a consistent and significant decreased mean heart rate in Akita mice starting at week 9, as shown in the top panel of figure 20, which indicates an altered autonomic function that begins at 2 month old Akita mice. We also observed some non-significant decrease in SDNN value in Akita mice after week 12. The SDNN parameter is reflective of the overall heart rate variability, and no consistent overall reduction in the autonomic function is observed with our data. The RMSSD also did not significantly change in Akita mice during the first half of the experiment, but in some weeks, RMSSD values showed a significant reduction. However, note that there was an increase in RMSSD values in week 19 in Akita. Therefore, results of both the SDNN and RMSSD are scattered and not consistent, leading to an inconclusive interpretation. The effectiveness and reliability of these two traditional parameters are thus questionable.

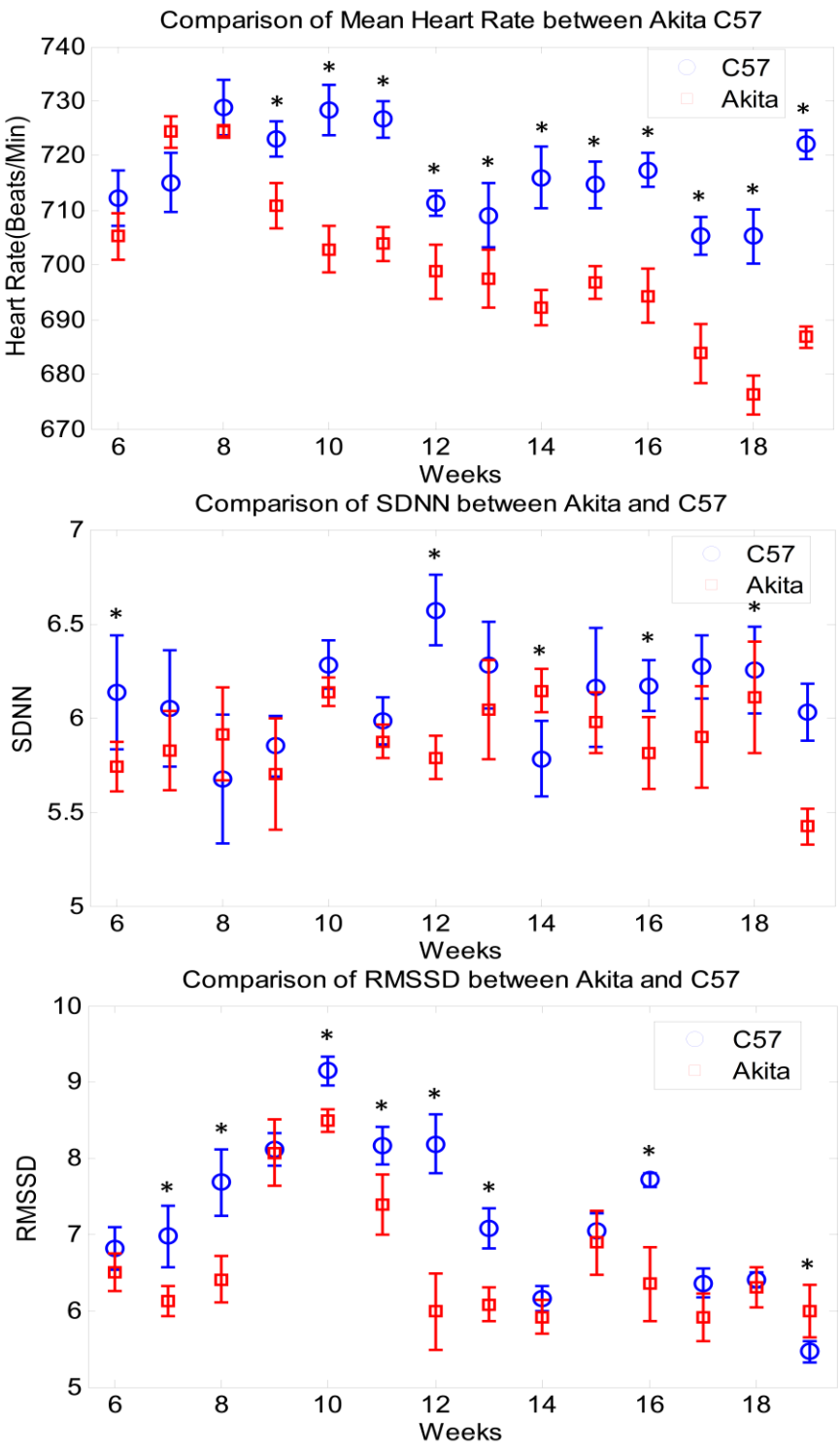

Figure 20, comparison of mean heart rate, SDNN, and RSSMD between C57 (n=5) and Akita (n=5) mice from 6 weeks old to 19 weeks old. * denotes statistical significance at $P < 0.05$

B. Frequency domain (spectral analysis) assessment of autonomic function.

In the frequency domain, LF and HF band spectral powers are used as an indicator of the sympathetic and parasympathetic activities. As shown in the top panel of figure 21, no significant changes in the normalized LF power were observed in Akita mice throughout the experiment (except for week 11) which implies that no sympathetic impairment can be found using this method. Meanwhile, the HF power did not change initially in Akita followed by a slight reduction on week 10 to week 18 but not in week 15, 17 and 19. Similar to RMSSD values, the difference between two strains is not consistent throughout the experiment. The lower HF power implies lower parasympathetic activities but apparently no consistent parasympathetic impairment can be concluded. We also estimated the autonomic balance by calculating the ratio between LF and HF. Results shown in figure 23 indicate that Akita mice did not have significant change in LF/HF ratio in comparison to C57 throughout the experiment.

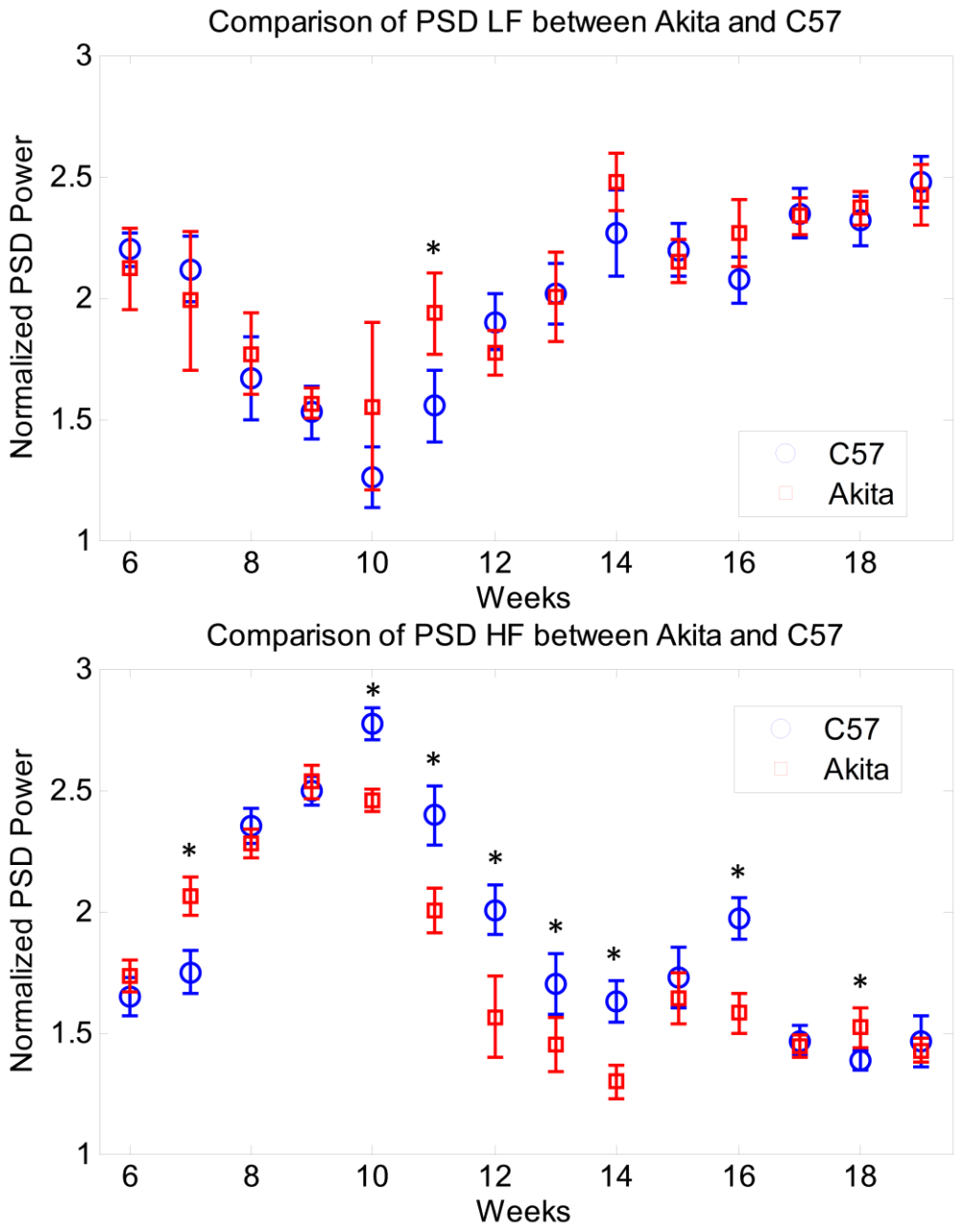

Figure 21, the top panel shows LF and HF power of PSD method; the top and bottom panel show the comparison of LF and HF power based on weekly basis; C57 (n=5); Akita n=5. * denotes statistical significance at $P < 0.05$

C. PDM analysis of sympathetic and parasympathetic activities.

As we have confirmed in the Specific Aims 2 and 3, the reduction of the autonomic function can be expected in 3 -4 month old Akita mice. However, as shown in the results section *B*, the linear frequency domain measures, namely the LF, HF and LF/HF ratio, all failed to discern differences in the sympathetic and parasympathetic dynamics, as well as the autonomic balance between Akita and C57, even for those mice that are 4 month old. This result is contradictory to what we have observed in the Specific Aims 2 and 3. Therefore, we used PDM because it is a nonlinear and nonstationary method that has been shown to provide more accurate characterization of the ANS function. As shown in the bottom panel of figure 22**,** the PDM-derived sympathetic power remains unchanged initially but then decreases from week 11 throughout the experiment in Akita mice. Such reduction became greater after the onset of the sympathetic impairment and then to the end of the experiment. This result suggests that depressed or impaired sympathetic activities are presented as early as 3 months in Akita and become more severe as they grow. On the contrary, the parasympathetic power via PDM shows no change for all time points. Note that mice were in an active state thus parasympathetic activities were already depressed, thus difference of the parasympathetic activities between Akita and C57 will not likely to occur. The Symp/Parasymp ratio also clearly indicates an autonomic imbalance starting at week 11 and then throughout the experiment. In this case, the autonomic imbalance in Akita is most likely due to decreased sympathetic activities since there was no significant change in the parasympathetic dynamics

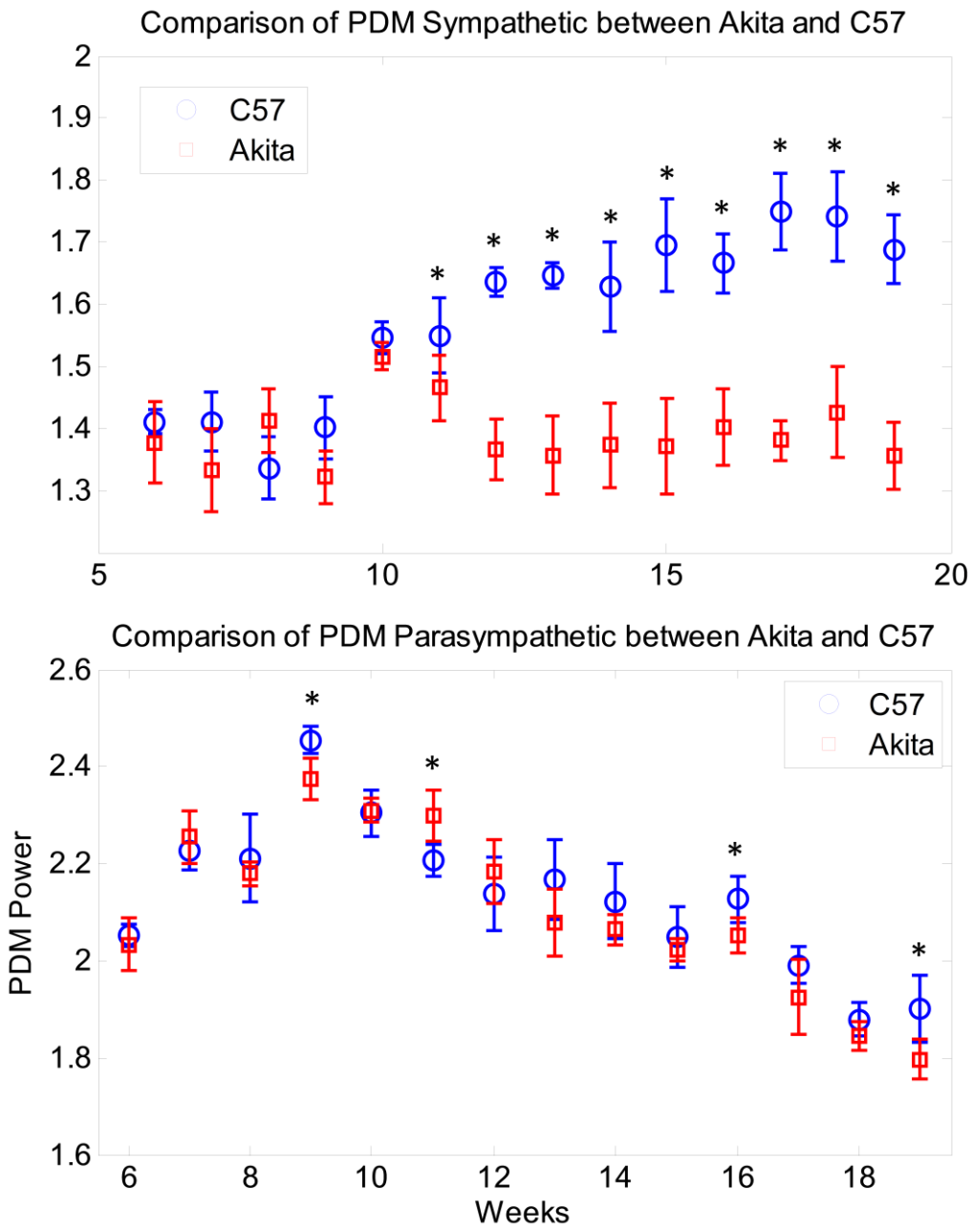

Figure 22, the top and bottom panel shows the sympathetic and parasympathetic dynamics extracted by PDM method; C57 (n=5); Akita n=5. * denotes statistical significance at $P < 0.05$

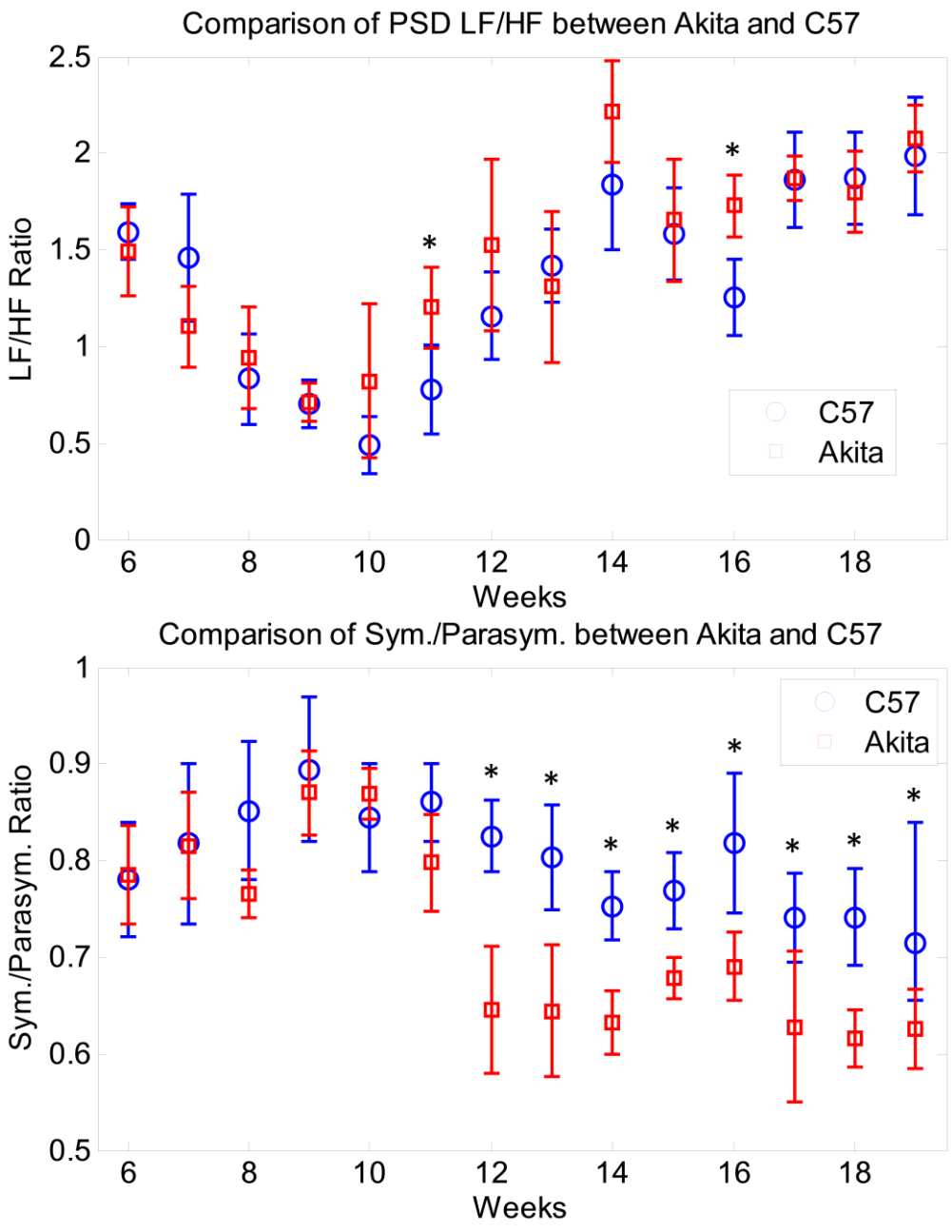

Figure 23, the top and bottom panel shows autonomic balance calculated by LF/HF ratio and PDM Sym./Parasym.; C57 (n=5); Akita n=5. * denotes statistical significance at $P < 0.05$

Summary

In this specific aim, we have examined the development of the ANS impairment on Akita mice from the age of 6 weeks to 19 weeks. The heart rate of Akita mice decreased starting from week 9 and maintained this trend throughout the experiment. The abnormal heart rate in Akita mice indicated a possible impaired autonomic function. By using the PDM method, we successfully found an impaired sympathetic function starting at week 11 and continued to deteriorate until the end of the experiment. However the parasympathetic power via PDM did not change most likely due to already depressed parasympathetic activities in conscious mice. Unlike the previous specific aims, the time and frequency domain parameters failed to characterize the altered ANS function in Akita mice using the pulse oximeter recordings. This observation may also stem from the fact that PPG are collected in alert animals and the stress they experienced created greater variability and complexity in the signal. It may be more difficult for the traditional linear and stationary methods to characterize the autonomic function.

DISCUSSION

Diabetic autonomic neuropathy (DAN) is a disease involving the entire autonomic nervous system and it is a common complication of diabetes. Cardiovascular autonomic neuropathy is one of the most studied and a clinical subset of DAN. Timely diagnosis of DCAN is needed as individuals with abnormal autonomic function are found to have a greater risk for severe hypoglycemia (10). Diagnosis of DCAN currently involves many different autonomic function tests and involves testing of RR variability, Valsalva maneuver and postural blood pressure testing. It has been suggested that regular HRV testing provides early detection of DCAN which subsequently can lead to timely therapeutic interventions (45). For example, it has been suggested that peripheral neuropathy can be reversed if timely detection and appropriate subsequent therapeutic interventions (such as inhibition of caspase-mediated pathway) are administered (46).

To this end, the goal of our present work is to demonstrate an alternative to the traditional HRV measures involving both time- and frequency-domain parameters which have been well documented to have many shortcomings. This was the case with our results as we found significantly increased parasympathetic dynamics as determined by the increased HF power as well as RMSSD values (see Table II**)** in Akita as compared to wildtype mice. The PDM, on the contrary, showed a significant decrease in the parasympathetic dynamics. The gold-standard approaches such as immunohistochemistry staining and Western blot analysis of mice heart clearly showed a significant decrease in the parasympathetic and sympathetic nerve densities in Akita as compared to wildtype mice, corroborating our PDM results. Thus, our current work demonstrates a more effective and sensitive approach to HRV analysis in the diagnosis of DCAN than the traditional HRV measures. The advantage of using PDM method over the traditional HRV measures has been already demonstrated in our previous study involving healthy subjects with the aid of pharmacological blockades (27).

We have primarily studied 4 month old Akita mice because peripheral neuropathy is known to occur after mice have reached this age. Our work suggests DCAN also occurs at 4 months old. However, researchers did not know if DCAN occurs earlier than 4 months. The Western Blot analysis implies autonomic dysfunction might occur before 4 month old such as 3 month old, thus, we are interested in investigating the onset of DCAN in Akita mice at younger ages. The main roadblock to recording telemetry ECG earlier than 4 months is that a telemetry sensor is too big and heavy (~5 gms). Note that a 1 month old Akita mouse weighs ~16 gms. To circumvent this limitation, we investigated the use of a tail-cuff PPG sensor as our results suggest that accurate RR intervals can be obtained in 1 month old mice. This allows us to monitor the progression and onset of DCAN in Akita mice.

By utilizing a noninvasive PPG sensor we avoided ECG sensor implantation surgeries and overcame many technical limitations associated with ECG data collection. In fact we were able to obtain signals from Akita mice that were as young as 1 month old. From the results, the long term heart rate monitoring suggests that Akita mice start to present their abnormal heart rate (lower than wildtype) at about 9 weeks old (2 month). Meanwhile, the PDM-derived sympathetic dynamics clearly showed the onset of the sympathetic function impairment and autonomic imbalance starting at 11 weeks. To date, the earliest reported diabetic neuropathy in Akita mice was observed at 4 month of age. Therefore our technique provides a promising potential for early diagnosis of DCAN.

Note that the Specific Aim 3 has shown evidence of parasympathetic nerve degeneration in Akita mice at 4 months old which was also confirmed with our signal processing approach as detailed in the Specific Aim 2. However, we did not observe PDM-derived parasympathetic impairment in the PPG recordings. This conflicting result may be due to the different state (alert v. quiet) of mice at which we collected data. Under an alert state, which was the condition of these experiments, the parasympathetic

activities are far more depressed in both strains of mice. Thus, the difference between Akita and C57 is likely to be minimal. In contrast, for the quiet state data, which was used in ECG recordings, the parasympathetic system was more enhanced thus, any difference will be more pronounced.

As a computational method, the technique we have developed can be easily implementable for clinical applications since ECG or PPG recordings are convenient and already widely used. Personal health is becoming more important for both diseased and healthy subjects. Our technique, which needs only a few minutes of ECG or PPG recordings, can provide an estimate of autonomic function in near real-time. With daily monitoring, diabetic patients will be able to keep track of their development of DCAN and receive prompt and proper medical care. Therefore this technique will potentially allow patients to better control DCAN condition; if detected early, there is a hope that DCAN be reversed.

For future clinical applications to be viable with PDM method for detection of DCAN, a threshold value of the ANS dynamics needs to be determined. Further, it is unknown if the autonomic function detected by PDM will be sensitive enough to distinguish DCAN subject from normal subject for all age groups. Even within the same age group, the sensitivity and specificity will require thorough investigation since human subjects have more complicated physiological conditions compared to mice. These are some of the obstacles that need to be overcome before the PDM can be utilized as a detector of DCAN in a clinical setting, or for home care diagnostic usage.

CONCLUSION

In this study, we developed a noninvasive HRV analysis approach suitable for mice applications. This approach is able to detect autonomic dysfunction based on HRV measurements. We employed this technique and analyzed long term telemetry ECG recordings from 4 month old mice to investigate autonomic dysfunction in diabetic mice. Traditional method for autonomic function assessment is based on time- and frequency-domain parameters of HRV. However, they are problematic mainly due to two reasons: 1. inaccuracy in separating the sympathetic and parasympathetic activities; 2. not accounting for nonlinearity in HRV signals. Our PDM technique overcomes these limitations and its performance was tested against the traditional methods. Our method PDM by design, overcome these two limitations and provided more accurate DCAN assessment than the conventional approaches.

ECG was measured via telemetry in conscious sex- and age- matched 4 month old C57/Bl6 controls and Akita mice. Our results indicate a significant cardiac autonomic impairment in the diabetic mice. Further, both immunohistochemical and Western blot analyses show a reduction in nerve density in Akita mice as compared to the control mice, thus, corroborating our PDM data analysis of HRV records. In order to monitor the long term progression of DCAN, the PPG data from 1 month old mice to 4 month old mice were also measured. Our method found the onset of the impaired autonomic function in Akita mice starting at 3 months. The long-term goal of this project is to develop this method to the point at which it can be used to detect DCAN in diabetic subjects.

FUTURE WORK

In Specific Aim 3 we have examined the expression of protein markers for autonomic nerves system in 2, 3, and 4 month old mice using Western blot analysis. The difference of autonomic nerves density found between Akita and C57BL6 mice corroborates our computational findings.,

In specific aim 3, we only visualized the overall nerve density reduction in 4 month old Akita mice using immunohistochemistry staining. The sympathetic and parasympathetic nerve densities will be further examined in 2 month, 3 month and 4 month old mice. This will further validate our computational analysis and Western blot results in 2, 3, and 4 month old mice.

So far, the computational results from conscious young mice (namely 2 and 3 month old) are derived only from PPG recordings, when they are in an active state. While the animals were in an active state, they were resrained in an immobilizer which can result in significant stress to animals. In other words, stress and fear can elevate the sympathetic nervous dynamics. The motion artifacts which is significant in active animals prevented us from obtaining accurate autonomic dynamics using ECG recordings. Thus, we had to resort to data analysis for those segments that were deemed to be in an inactive state. The above described scenarios may have resulted in contradictory results in the 4 month old mice using ECG and PPG recordings.. As a part of future work, One possible solution to overcome the difference seen is to use blood pressure recordings as the pressure sensor is applicable to even 2 month oldmice. Note that RR interval can be derived from blood pressure data.

As discussed in the previous section, further steps need to be taken before future clinical use can be realized. Our technique is noninvasive and only requires a few minutes of ECG, contiuous blood pressure or PPG recordings, which makes it easier to satisfy FDA regulations. Once approved by FDA, we will need to thoroughly investigate our technique for human

applications. Proper threshold of DCAN for human subjects needs to be obtained, which will probably be variable for different age groups. Moreover, the sensitivity and specificity also need to be established for human subjects.

There are some other potential applications of our technique. One such application is to use a smart phone to collect RR intervals (47). It has been shown that a video camera that resides on a smart phone can be used to capture heart rate fluctuations (47). Once a proper threshold for DCAN is obtained, our technique can be implemented into a smart phone. Diabetic patients will be allowed to monitor their development or detection of DCAN at their leisure in their homes by taking a few minute of PPG recordings using a smart phone. The convenience and efficiency of this technique has the potential to significantly impact the diagnostics of DCAN which has not been possible to date.

REFERENCE

1. Kennedy JM, Zochodne DW. Experimental diabetic neuropathy with spontaneous recovery: is there irreparable damage? Diabetes. 2005;54(3):830-7.

2. Heart rate variability: standards of measurement, physiological interpretation and clinical use. Task Force of the European Society of Cardiology and the North American Society of Pacing and Electrophysiology. Circulation. 1996;93(5):1043-65.

3. Zhong Y, Jan KM, Ju KH, Chon KH. Quantifying cardiac sympathetic and parasympathetic nervous activities using principal dynamic modes analysis of heart rate variability. Am J Physiol Heart Circ Physiol. 2006;291(3):H1475-83.

4. Mortara A, Sleight P, Pinna GD, Maestri R, Prpa A, La Rovere MT, et al. Abnormal awake respiratory patterns are common in chronic heart failure and may prevent evaluation of autonomic tone by measures of heart rate variability. Circulation. 1997;96(1):246-52.

5. Salvemini D, Mazzon E, Dugo L, Serraino I, De Sarro A, Caputi AP, et al. Amelioration of joint disease in a rat model of collagen-induced arthritis by M40403, a superoxide dismutase mimetic. Arthritis Rheum. 2001;44(12):2909-21.

6. Maser RE, Lenhard MJ. Cardiovascular autonomic neuropathy due to diabetes mellitus: clinical manifestations, consequences, and treatment. J Clin Endocrinol Metab. 2005;90(10):5896-903.

7. Iizuka S, Suzuki W, Tabuchi M, Nagata M, Imamura S, Kobayashi Y, et al. Diabetic complications in a new animal model (TSOD mouse) of spontaneous NIDDM with obesity. Exp Anim. 2005;54(1):71-83.

8. Vinik AI, Freeman R, Erbas T. Diabetic autonomic neuropathy. Semin Neurol. 2003;23(4):365-72.

9. Huikuri HV, Koistinen MJ, Yli-Mayry S, Airaksinen KE, Seppanen T, Ikaheimo MJ, et al. Impaired low-frequency oscillations of heart rate in patients with prior acute myocardial infarction and life-threatening arrhythmias. Am J Cardiol. 1995;76(1):56-60.

10. Koivikko ML, Salmela PI, Airaksinen KE, Tapanainen JS, Ruokonen A, Makikallio TH, et al. Effects of sustained insulin-induced hypoglycemia on cardiovascular autonomic regulation in type 1 diabetes. Diabetes. 2005;54(3):744-50.

11. Davies CT NJ. Sinus arrhythmia in man at rest. J Appl Physiol. 1967;22:947-55.

12. Bigger JT, Jr., Fleiss JL, Steinman RC, Rolnitzky LM, Schneider WJ, Stein PK. RR variability in healthy, middle-aged persons compared with patients with chronic coronary heart disease or recent acute myocardial infarction. Circulation. 1995;91(7):1936-43.

13. Ziegler D, Gries FA, Spuler M, Lessmann F. The epidemiology of diabetic neuropathy. Diabetic Cardiovascular Autonomic Neuropathy Multicenter Study Group. J Diabetes Complications. 1992;6(1):49-57.

14. Schroeder EB, Chambless LE, Liao D, Prineas RJ, Evans GW, Rosamond WD, et al. Diabetes, glucose, insulin, and heart rate variability: the Atherosclerosis Risk in Communities (ARIC) study. Diabetes Care. 2005;28(3):668-74.

15. Howarth FC, Jacobson M, Shafiullah M, Adeghate E. Long-term effects of streptozotocin-induced diabetes on the electrocardiogram, physical activity and body temperature in rats. Exp Physiol. 2005;90(6):827-35.

16. Howarth FC, Jacobson M, Shafiullah M, Adeghate E. Effects of insulin treatment on heart rhythm, body temperature and physical activity in streptozotocin-induced diabetic rat. Clin Exp Pharmacol Physiol. 2006;33(4):327-31.

17. Choeiri C, Hewitt K, Durkin J, Simard CJ, Renaud JM, Messier C. Longitudinal evaluation of memory performance and peripheral neuropathy in the Ins2C96Y Akita mice. Behav Brain Res. 2005;157(1):31-8.

18. Suzuki W, Iizuka S, Tabuchi M, Funo S, Yanagisawa T, Kimura M, et al. A new mouse model of spontaneous diabetes derived from ddY strain. Exp Anim. 1999;48(3):181-9.

19. Boudina S, Abel ED. Mitochondrial uncoupling: a key contributor to reduced cardiac efficiency in diabetes. Physiology (Bethesda). 2006;21:250-8.

20. Koulmanda M, Qipo A, Auchincloss H, Jr., Smith RN. Effects of streptozotocin on autoimmune diabetes in NOD mice. Clin Exp Immunol. 2003;134(2):210-6. PMCID: 1808849.

21. Schmidt RE, Green KG, Snipes LL, Feng D. Neuritic dystrophy and neuronopathy in Akita (Ins2(Akita)) diabetic mouse sympathetic ganglia. Exp Neurol. 2009;216(1):207-18. PMCID: 2672346.

22. Araki E, Oyadomari S, Mori M. Impact of endoplasmic reticulum stress pathway on pancreatic beta-cells and diabetes mellitus. Exp Biol Med (Maywood). 2003;228(10):1213-7.

23. Eckberg DL. Sympathovagal balance: a critical appraisal. Reply. Circulation. 1998;98(23):2643-4.

24. Howarth FC, Jacobson M, Naseer O, Adeghate E. Short-term effects of streptozotocin-induced diabetes on the electrocardiogram, physical activity and body temperature in rats. Exp Physiol. 2005;90(2):237-45.

25. Bigger JT, Jr., Fleiss JL, Rolnitzky LM, Steinman RC, Schneider WJ. Time course of recovery of heart period variability after myocardial infarction. J Am Coll Cardiol. 1991;18(7):1643-9.

26. Boer-Martins L, Figueiredo VN, Demacq C, Martins LC, Consolin-Colombo F, Figueiredo MJ, et al. Relationship of autonomic imbalance and circadian disruption with obesity and type 2 diabetes in resistant hypertensive patients. Cardiovasc Diabetol. 2011;10:24.

27. Zhong YR, Jan KM, Ju KH, Chon KH. Quantifying cardiac sympathetic and parasympathetic nervous activities using principal dynamic modes analysis of heart rate variability. Am J Physiol-Heart C. 2006;291(3):H1475-H83.

28. Zhong Y, Wang H, Ju KH, Jan KM, Chon KH. Nonlinear analysis of the separate contributions of autonomic nervous systems to heart rate variability using principal dynamic modes. IEEE Trans Biomed Eng. 2004;51(2):255-62.

29. Wang H, Siu K, Ju K, Chon KH. A high resolution approach to estimating time-frequency spectra and their amplitudes. Ann Biomed Eng. 2006;34(2):326-38.

30. Marmarelis VZ. Identification of nonlinear biological systems using Laguerre expansions of kernels. Ann Biomed Eng. 1993;21(6):573-89.

31. Zou R, Chon KH. Robust algorithm for estimation of time-varying transfer functions. IEEE Trans Biomed Eng. 2004;51(2):219-28.

32. Li F, Drel VR, Szabo C, Stevens MJ, Obrosova IG. Low-dose poly(ADP-ribose) polymerase inhibitor-containing combination therapies reverse early peripheral diabetic neuropathy. Diabetes. 2005;54(5):1514-22.

33. Wada R, Yagihashi S. Nitric oxide generation and poly(ADP ribose) polymerase activation precede beta-cell death in rats with a single high-dose injection of streptozotocin. Virchows Arch. 2004;444(4):375-82.

34. Yun WH, Min SW, Huh J, Ro YJ, Kim CS. Autonomic changes in preoperative uncomplicated diabetic patients with postural changes. J Int Med Res. 2010;38(5):1764-71.

35. Feldman EL. Oxidative stress and diabetic neuropathy: a new understanding of an old problem. J Clin Invest. 2003;111(4):431-3. PMCID: 151930.

36. Petrecca K, Shrier A. Spatial distribution of nerve processes and beta-adrenoreceptors in the rat atrioventricular node. J Anat. 1998;192 (Pt 4):517-28. PMCID: 1467806.

37. Yamamoto K, Vernier P. The evolution of dopamine systems in chordates. Front Neuroanat. 2011;5:21. PMCID: 3070214.

38. Flores-Otero J, Davis RL. Synaptic proteins are tonotopically graded in postnatal and adult type I and type II spiral ganglion neurons. J Comp Neurol. 2011;519(8):1455-75.

39. Tu JL, Zhao CB, Vollmer T, Coons S, Lin HJ, Marsh S, et al. APOE 4 polymorphism results in early cognitive deficits in an EAE model. Biochem Biophys Res Commun. 2009;384(4):466-70.

40. Masliukov PM, Timmermans JP. Immunocytochemical properties of stellate ganglion neurons during early postnatal development. Histochem Cell Biol. 2004;122(3):201-9.

41. Yamamoto M, Dobrzynski H, Tellez J, Niwa R, Billeter R, Honjo H, et al. Extended atrial conduction system characterised by the expression of the HCN4 channel and connexin45. Cardiovasc Res. 2006;72(2):271-81.

42. Lu G, Yang F, Taylor JA, Stein JF. A comparison of photoplethysmography and ECG recording to analyse heart rate variability in healthy subjects. J Med Eng Technol. 2009;33(8):634-41.

43. Wagner JL, Ruskin KJ. Pulse oximetry: basic principles and applications in aerospace medicine. Aviat Space Environ Med. 2007;78(10):973-8.

44. Gil E, Orini M, Bailon R, Vergara JM, Mainardi L, Laguna P. Time-varying spectral analysis for comparison of HRV and PPG variability during tilt table test. Conf Proc IEEE Eng Med Biol Soc. 2010;2010:3579-82.

45. Andrew J.M. Boulton AIV, MD, Joseph C. Arezzo, . Diabetic Neuropathies: A Statement by the ADA: Diagnostic Criteria and Brief Clinical Aspects. Diabetes Care. 2005;28(4):956-62.

46. Shanthi Srinivasan MS, and John W. Wiley. Diabetic Peripheral Neuropathy: Evidence for Apoptosis and Associated Mitochondrial Dysfunctio. Diabetes. 2000;49:1932-8.

47. Oresko JJ, Duschl H, Cheng AC. A wearable smartphone-based platform for real-time cardiovascular disease detection via electrocardiogram processing. IEEE Trans Inf Technol Biomed. 2010;14(3):734-40.